DOE/NASA/0241-3
NASA CR-165568

DEVELOP AND TEST FUEL CELL POWERED ON-SITE INTEGRATED TOTAL ENERGY SYSTEMS: PHASE III, FULL-SCALE POWER PLANT DEVELOPMENT

3RD QUARTERLY REPORT: AUGUST - OCTOBER, 1981

ENGELHARD INDUSTRIES DIVISION
ENGELHARD CORPORATION
EDISON, NJ 08818
A. Kaufman, Contract Manager
G. K. Johnson, Contract Technical Coordinator

REPORT DATE: April 28, 1982

PREPARED FOR
NATIONAL AERONAUTICS AND SPACE ADMINISTRATION
LEWIS RESEARCH CENTER
UNDER CONTRACT DEN3-241

for
U.S. DEPARTMENT OF ENERGY
ENERGY TECHNOLOGY
DIVISION OF FOSSIL FUEL UTILIZATION
UNDER INTERAGENCY AGREEMENT DE-AI-01-80ET17088

DOE/NASA/0241-3
NASA CR-165568

DEVELOP AND TEST FUEL CELL POWERED ON-SITE INTEGRATED TOTAL ENERGY SYSTEMS: PHASE III, FULL-SCALE POWER PLANT DEVELOPMENT

3RD QUARTERLY REPORT: AUGUST - OCTOBER, 1981

ENGELHARD INDUSTRIES DIVISION
ENGELHARD CORPORATION
EDISON, NJ 08818
A. Kaufman, Contract Manager
G. K. Johnson, Contract Technical Coordinator

REPORT DATE: April 28, 1982

PREPARED FOR
NATIONAL AERONAUTICS AND SPACE ADMINISTRATION
LEWIS RESEARCH CENTER
UNDER CONTRACT DEN3-241

for
U.S. DEPARTMENT OF ENERGY
ENERGY TECHNOLOGY
DIVISION OF FOSSIL FUEL UTILIZATION
UNDER INTERAGENCY AGREEMENT DE-AI-01-80ET17088

SECTION I. INTRODUCTION

Engelhard's objective under the present contract is to contribute substantially to the national fuel conservation program by developing a commercially viable and cost-effective phosphoric acid fuel cell powered on-site integrated energy system (OS/IES). The fuel cell offers energy efficiencies in the range of 35-40% of the higher heating value of available fuels in the form of electrical energy. In addition, by utilizing the thermal energy generated for heating, ventilating and air-conditioning (HVAC), a fuel cell OS/IES could provide total energy efficiencies in the neighborhood of 80%. Also, the Engelhard fuel cell OS/IES, which is the objective of the present program, offers the important incentive of replacing imported oil with domestically produced methanol, including coal-derived methanol.

Engelhard has successfully completed the first two phases of a five-phase program. The next three phases entail an integration of the fuel cell system into a total energy system for multi-family residential and commercial buildings. The mandate of Phase III is to develop a full scale 50kW breadboard power plant module and to identify a suitable type of application site. Toward this end, an initial objective in Phase III is to complete the integration and testing of the 5kW system whose components were developed during Phase II. Following the test of this sub-scale system, scale-up activities will be implemented as a total effort. Throughout this design and engineering program, continuing technology support activity will be maintained to assure that performance, reliability, and cost objectives are attained.

SECTION II. TECHNICAL PROGRESS SUMMARY

TASK I - 5kW POWER SYSTEM DEVELOPMENT (97046)

This task is of limited duration and has as its objective the complete integration of 5kW components developed during Phase II. This integrated 5kW system is automated under microprocessor control. At the present time the system is fully assembled and has been tested on a limited basis as described below. The 5kW stack does not perform to specifications because of partially defective ABA bipolar plates which allow some leakage of reactant gases. (Refer to August, 1981 Monthly Technical Progress Narrative, pp. 3-4, for details.) The production problem with the ABA plates is believed to be solved as outlined later in this report under Section II, Task IV. A rebuild of the stack is scheduled for the end of 1981.

An updated schematic of the integrated system is shown in Figure 1. Several minor changes have been made since this schematic was first presented in the Quarterly Report for May-July, 1981. Normally-open solenoid valves S3 and S4 were added to provide for automatic purging of the stack and reformer with nitrogen in an emergency. Any set of conditions programmed to shut down the entire system will trigger the nitrogen purge. Relief valves RV2 and RV3 were added to set an upper limit on methanol and methanol/water delivery pressures. A bleed valve BV1 was also added to the cooling system loop. Other component codes were shown in Table II, and flow rates at important nodes in Table I of the previous Quarterly Report.

The layout of system components on two moveable carts is shown in Figure 2. This arrangement allows easy access for servicing and also provides portability.

SECTION II. - CONTINUED

Tests were run on the 5kW system at Engelhard's Fuel Cell Test Facility at Union, New Jersey. Operation was limited to about 2kW power due to limitations of the stack described above. It was possible, however, to check many operational features of the integrated system. In general the microprocessor control system worked very well.

Successful checks of the following operational features were made:

A. Control Mode 13: Fuel cell preheat at various temperatures from 394 to 477 K (250 to 400°F).

B. Control Mode 15: Automatic fuel cell operation using an outside hydrogen source.

C. Control Mode 16: Automatic operation of the reformer.

D. Control Mode 11: Fully automatic operation of the complete system at preset control points.

While in Mode 11, power curves were generated at two fuel cell temperatures as shown in Figure 3. These data were taken without recycling the fuel cell anode vent gas back to the reformer. When this recycle loop was closed, the lower curves in Figure 4 were obtained. The reason for the lower voltages and power values when operated with the closed loop was that this closure increased the pressure at the anode side of the fuel cell and, thereby, increased the reactant leakage in the stack.

Further testing of this system will be deferred until the stack is rebuilt.

SECTION II. - CONTINUED

TASK II - ON-SITE SYSTEM APPLICATION ANALYSIS (97047)

The purpose of this task is to develop an application model for on-site integrated systems, with some emphasis on a system of 50kW (electrical) modular capability. The model will consider fuel availability and costs, building types and sizes, power distribution requirements (electrical and thermal), waste heat utilization potential, types of ownership of the OS/IES, and grid connection vs. stand-alone operation. The work of this task is being carried out under sub-contract by Arthur D. Little, Inc.

A.D.L. is nearing completion of an economic feasibility analysis of a fuel cell OS/IES for one building type (a retail store in Washington, D.C.). Details and results of this analysis are due at the end of November. In addition, at that time, A.D.L. will recommend several other building types for further study. They plan to study one building type in multiple climatic zones, and with multiple electric rate structures.

A.D.L. has recently reviewed and summarized the federal regulations that determine if a utility customer is a qualified cogenerator. The following is an excerpt of their summary:

> The FERC has issued its final rules under Section 210 of PURPA. Two types of rules have been instituted, those for small power producers using renewable energy resources like wind and water, and those for cogenerators using fossil fuel sources. The rules for cogenerators using coal as their primary energy source are different from those using fuels based on oil and natural gas. Both sets of rules have a measure of efficiency as part of the definition. The argument was that a small power producer using only a minute portion of the waste heat (to heat a tool shed) should not be considered a qualified cogenerator; the use of waste heat under these circumstances would correspond to a legal fiction, and should not be tolerated. This provision is even more important when applied to cogenerators using oil and natural gas as their energy source.

SECTION II. - CONTINUED

There are two types of cogeneration equipment which must be covered by the efficiency standards. They are:

- Cogeneration equipment like diesels and fuel cells, which produce thermal energy as a by-product of producing electrical energy: thermal supply is coincident with the electrical supply for these systems; and
- The steam extraction turbines where useful thermal energy is removed from the turbine before it is used to produce electricity; thermal supply and the electrical supply are anti-coincident for these systems (when the thermal supply is high, the electrical supply is low and vice versa).

Because the rules must apply to both types of cogeneration equipment, the equations must be written in terms of annual average energy rather than instantaneous energy delivered. The equations representing the efficiency standards have the following form:

$$\bar{E}_t \geq .05 \left[\bar{E}_e + \bar{E}_t\right] \tag{1}$$

and

$$\bar{E}_e + \frac{\bar{E}_t}{2} \geq \begin{cases} .425\ \bar{E}_{in} \text{ if } \bar{E}_t \geq .15 \left[\bar{E}_e + \bar{E}_t\right] & (2) \\ .45\ \bar{E}_{in} \text{ if } \bar{E}_t \leq .15 \left[\bar{E}_e + \bar{E}_t\right] & (3) \end{cases}$$

Where: $\bar{E}_{in}$ is the average total fuel energy into the system

$\bar{E}_t$ is the average thermal energy

$\bar{E}_e$ is the average electrical energy

The expression of the standard in terms of annual averages leads to a difficult design problem for the fuel cell cogeneration equipment. In order to be considered a qualified cogenerator during the time when the thermal demand of the building is low, a higher percentage of the available thermal energy must be used during the peak demand season than would be otherwise required if the equations referred to instantaneous energy usage.

SECTION II. - CONTINUED

If we assume a heat rate for the fuel cell as 9729 kJ per kwh, and if Equation 2 were to apply instantaneously, this would imply that a minimum of 1072 kJ of thermal energy must be used for every kwh of electricity produced. If Equation 3 applied instantaneously, a minimum of 1558 kJ must be used for every kwh produced. However, if either of these numbers were used as the design parameter, the cogenerator might not be a qualified cogenerator except during the winter and summer seasons. In order to be a qualified cogenerator during the entire season, more of the waste heat must be used.

The benefits that accrue from meeting the criteria of a qualified cogenerator include:

- The provision, by the utility, of back-up capacity, with charges which are identical to the charges that would have applied if the customer were not a cogenerator, and
- The purchase of the excess electrical energy at a rate not to exceed the utility's avoided cost of service.

While there was a great deal of argument concerning what constituted reasonable back-up capacity prior to the issuance of the FERC rules, this argument is now settled. However, argument continues concerning what constitutes the utility's avoided costs.

TASK III - ON-SITE SYSTEM DEVELOPMENT

This task forms the core of the Phase III Contract. Work under this task will result in the breadboard design of a system for an on-site application. The power plant will be designed for a rated output of 50kW (electrical) or some multiple thereof. The fuel processor and power conditioner will each be 50kW modules, while the 50kW fuel cell will comprise two 25kW stack modules. This task is accordingly broken down into four sub-tasks as follows:

3.1 Large Stack Development (97048)
3.2 Large Fuel Processor Development (97038)
3.3 Overall System Analysis (97051)
3.4 Overall System Design and Development (97064)

SECTION II. - CONTINUED

A large part of Sub-Task 3.3 is being carried out by Physical Sciences Inc. (PSI) under subcontract.

LARGE STACK DEVELOPMENT (97048)

The preliminary design for the 25kW stack was completed in October and detailed drawings are approximately 20% complete. An overall sketch is shown in Figure 5. The cell size of 0.33m x 0.56m (13" x 22") will have an active, current-producing area of 0.30m x 0.53m (12" x 21") or $0.16m^2$ ($1.75 ft^2$).

To keep weight to a minimum, aluminum will be used for the stand, the compression plates and all manifolds.

The air and hydrogen manifolds will all be separate; each will consist of a frame with a removable cover for inspection. They will be independently sealed to prevent any cross-leakage of gases.

On previous Engelhard stacks the coolant manifolds have been mounted inside the air-inlet manifold. In the present 25kW design the coolant manifolds will be mounted entirely externally on the air-inlet side. Cooling plate inlet and exit tubes will be routed at corners between the separately sealed manifolds. This will allow for easier access to the cooling system.

In its present conception the stack will have 152 cells in 38 sub-stacks of four cells each. There will be a cooling plate between each pair of sub-stacks and an aluminum current collector at each end of the stack. In Figure 5 the stack height has been omitted. This dimension is subject to some variation depending upon the exact thickness eventually chosen for several components. The following is

SECTION II. - CONTINUED

an estimate of stack height based upon current technology:

152 cells at 0.293"	= 44.5"
37 cooling plates at 0.280"	= 10.4"
2 compression plates at 1.0"	= 2.0"
2 insulating plates at 0.125"	= 0.3"
2 current collector plates at 0.500"	= 1.0"
	58.2"
	(1.48 meters)

A variable-stack test fixture has been designed for forthcoming tests on full-size cells (0.33m x 0.56m or 13" x 22"). An undimensioned sketch of this unit is shown in Figure 6. Stacks of from one to 24 full-size cells will be accommodated by means of sliding seals on the manifold. Other details shown are the arrangement of manifold clamps at the corners and the adjustable stack compression plate and bolting design. Construction will be of mild steel, with the exception of the manifolds and current-collector plates, which will be of aluminum..

LARGE FUEL PROCESSOR DEVELOPMENT (97038)

The objective of Sub-Task 3.2 is to design a fuel processor for a 50kW fuel cell. This processor design will be based in part on the 5kW fuel processor design used in Task I.

The 5kW unit consists of 20 tubes 2.5 cm in diameter and 71 cm long. The catalyst in the tubes is heated by flue gas flowing through the shell of the reactor. The burner producing this flue gas is located directly below the shell and tube arrangement and is an integral part of the reformer vessel. The burner flue gas travels to the shell by way of a central duct. The revised version of the 5kW reformer is shown in Figure 7. This reformer has been evaluated as part of the 5kW integrated system and has met the requirements of that system.

SECTION II. - CONTINUED

Two key observations made during the evaluation of the 5kW unit are of interest in the design of the 50kW fuel processor. These are listed below:

1) The 5kW fuel processor was operated successfully at 150% of the design rate. That is, the present design could satisfy the hydrogen requirements of a 7.5 kW fuel cell. Part of this over-design might be desirable to allow for long-term aging. However, it could suggest that the scale-up factor for a 50 kW fuel processor need not be 10/1 but might be 50/7.5 or 6.7/1. It is important for various reasons, such as cost and load following, not to overdesign the 50kW fuel processor.

2) The reheating effect resulting from the interaction between the burner and the heat exchanger tubes of the reformer was reduced, but not entirely eliminated in the revised version of the 5kW fuel processor. Complete decoupling is desirable in order to minimize the CO level, which is affected by the catalyst bed exit temperature.

These considerations have led to a proposed 50kW fuel processor design that is shown schematically in Figure 8. This is only the first pass at a 50kW fuel processor design and other design problems must be resolved before a final design is established from which to order parts and to prepare shop drawings. The key elements of this design are outlined below:

1) The design is based on the concepts proven in the 5kW fuel processor.

2) The burner has been separated from the reactor. Figure 8 shows the burner adjacent to the reactor, but other locations will be considered to conserve heat and to minimize space requirements.

SECTION II. - CONTINUED

3) The straight-through (upflow) design lowers the flue gas pressure drop, since the flue gas makes fewer turns in passing through the reactor section, when compared to the 5kW reformer.

The process gas ($MeOH/H_2O$) also travels in the upward direction. This could be a problem at high gas velocities due to possible fluidization of the catalyst bed. However, Engelhard has licensed several upflow reactors which have been successfully demonstrated commercially. A proprietary design retains the catalyst. Also, the linear velocities in our design are well below the minimum fluidization velocity.

4) The reactor is a commercial shell-and-tube heat exchanger. For initial production, these will be less expensive than reactors built in-house. The heat-exchanger manufacturers are set up to build units with 3/4" and 1" tubes on a large volume basis. Larger diameter tubes actually increase cost, even though fewer tubes are required.

5) The burner is also a commercial unit capable of burning both anode vent gas and methanol. The burner contains two separate heat-exchanger coils; one to utilize waste-heat for heating, ventilating, and air-conditioning purposes and the second to preheat the methanol/water mixture to reactor inlet conditions. The first coil could also be used for heating a liquid for HVAC purposes. A key objective is control of the flue-gas temperature before it enters the tubular zone containing the catalyst. In the current 5kW reformer the flue-gas temperature is controlled primarily by excess air. This, however, lowers overall system efficiency since the heat content of the flue gas is not utilized to the maximum extent.

SECTION II. - CONTINUED

Design of the 50kW unit will utilize the mathematical models that are now available:

1) Steady-State System Model (PSI)
2) One-Dimensional Reactor Model
3) Two-Dimensional Reactor Model

The first two models were developed in Phase II and have been previously described. The system model establishes the design flow rates, etc. The one-dimensional model is used routinely to compare catalysts, reactor operating parameters, etc. The two-dimensional model is based on one purchased from the University of Arizona which involves the thesis work of Professor James Lowell Kuester*. This program has been transferred to Engelhard's DEC 11/34 computer and extensively modified to model tubular reactors of the type currently being used.

This two-dimensional model cuts the tube radius into 5 concentric annular cells in which transport properties (heat and mass) are propagated radially and axially to adjacent cells. As will be shown by some examples discussed below, the temperatures near the center of the tube, for the endothermic reaction, are considerably lower than those at the tube wall, resulting in lower rate of reaction. This model, therefore, gives a more accurate model of temperature and concentrations along the axis of the tube than does the one-dimensional model.

The use of the two-dimensional model in the development of the 50kW reformer will be illustrated by comparing the performances of reactors containing 2.54 cm (1") diameter tubes and 5.08 cm (2")

---

* Kuester, J. L., Two-Dimensional Model Simulation of Fixed Bed Catalytic Reactors, Doctoral Dissertation, Texas A&M University, College Station, Texas, January 1970.

diameter tubes. In this example the catalyst volume is the same for the two different tube sizes, as is the reactor length of 127 cm (4.2 ft). There are 120 tubes in the 2.54 cm version and only 27 tubes in the 5.08 cm version. Entrance conditions are identical for the two cases. Figure 9 shows the radial temperature differences, i.e., the difference between the center cell and the outermost radial cell, down the length of the tube. These differences go through a peak near the inlet of the tube. This maximum radial gradient is about 50°F (28 K) for the 5.08 cm tube and about 25°F (14 K) for the 2.54 cm tube. Even near the exit of the tube, large radial gradients are noted for the 5.08 cm tube. Figures 10 and 11 show the effects of these severe radial gradients on conversion through the tubes. At the inlets of the tubes, shown in Figure 10, the conversion starts to lag behind for the 5.08 cm tube. Figure 11 shows that the 2.54 cm tube achieves nearly 100% conversion at the 127 cm distance whereas the 5.08 cm tube approaches only 95% conversion of methanol. Calculations using the two-dimensional model show that a tube 254 cm long would be required to approach 100% conversion if the 5.08 cm tube were used.

A key parameter in both the one- and two-dimensional reactor models is the heat transfer coefficient called H_w. H_w is the overall coefficient for the inside film, the tube wall, and the outside (flue gas) film. In Figures 9, 10 and 11, the value used for H_w was 20.5 kJ/hr m^2 K. However, various calculations indicate a somewhat higher value for H_w. Calculations show that the 5.08 cm tube length required for essentially complete conversion could be cut in half if H_w were doubled. The value of H_w is affected by baffle arrangement, reactor configuration, and tube diameter. It varies axially within the shell as a function of temperature. A key objective in the experimental part of this program is to provide estimates of the value of H_w.

SECTION II. - CONTINUED

One approach to the determination of H_w is through simulation with single-tube studies. To this end, a 2" diameter tube has been assembled with thermocouples to measure axial and radial temperatures. Some preliminary runs have been made, and under some conditions radial gradients in excess of 100°F (56 K) have been obtained. Analysis of data from these runs is in progress.

Another aspect of the development of the 50kW reformer is the selection of catalyst. This will be discussed under Task V but must be considered in processor development since catalyst properties, in particular temperature limitations, impact reactor design and operation.

The program for the next quarter will be directed towards detailing the design of the 50kW unit as shown in Figure 8. This includes:

1) Contacts with heat-exchanger vendors to get cost and other data. Information on heat exchangers for both 5 and 50kW reformers is being requested. A 5kW unit would be tested to provide the most applicable scale-up data.

2) Contacts with burner manufacturers will be initiated also.

3) The single-tube studies will continue. The experimental results will be compared to the results from the two-dimensional model.

4) Ancillary components will be sized.

SECTION II. - CONTINUED

OVERALL SYSTEM ANALYSIS (97051)

The objective of this sub-task is to maximize overall fuel utilization and to minimize installed cost. This will be assisted by use of a computer model of the power plant and interfacing elements. As required, various items of the HVAC subsystem will be modeled. Physical Sciences Incorporated is developing these models with Engelhard.

Last quarter the reporting concerned various sub-routines that were being developed or improved to aid in this analysis. During this quarter work has focused on three areas:

1) The Advantages of Pressurization
2) System Efficiency at Part Load
3) HVAC Modules

The last item is still being developed. An important part of that work was to develop a module to handle heat and mass transfer simultaneously as, for example, in a condenser. More details of this work will be presented later.

The advantages of pressurizing a fuel cell power plant are listed in Table I. Improvements in system efficiency and reduction in power plant costs are attainable. Turbochargers of about the size required for a 50kW unit are commercially available for automotive use; the fuel cell power plant will require about 4.5 m^3/minute of air for burning the anode vent gas and for cathode feed. A system configuration for an on-site system is shown in Figure 12. The turbocompressor supplies air to the cathode and the two burners. This power plant supplies the fuel cell coolant to the HVAC subsystem at 483 K (410°F) and receives it back from HVAC at 434K (322°F). The condenser removes

sufficient water from the exhaust gas stream to supply the 1.3 moles of water required for each mole of methanol consumed.

Case studies were run at 1, 1.5, and 2 atmospheres. For a given set of conditions Figure 13 shows an increase in overall electrical efficiency from 31% to about 37% as pressure increases. Figure 14 shows the corresponding reduction in stack area that also results from pressurization. System cost is, of course, a strong function of stack area. Other studies are in progress with this system. The printout from the case studies has been expanded to list the cogeneration enthalpy available and to give more details about the turbine.

Plant efficiency at part load is an important characteristic of power plants. One advantage of fuel cells compared with other power plants such as gas turbines is that overall efficiency remains fairly constant with load. The computer programs must be able to determine this efficiency and to predict part load performance accurately.

In a fuel cell, overall efficiency is the product of the various subsystem efficiencies:

$$EO = \text{Overall Efficiency} = EM \cdot EI \cdot EF \cdot ES$$

where EM = Mechanical Efficiency
EI = Inverter Efficiency
EF = Fuel Processor Efficiency
ES = Stack (Fuel Cell) Efficiency

SECTION II. - CONTINUED

EM, EI, and EF tend to increase with load. The inverter efficiency for a 50kW system is expected to increase roughly from 80 to 90% as load increases from 25 to 75%, with little further increase for loads between 75 and 100%. However, ES decreases with increasing load since:

$$ES = V_{CELL}/1.2527$$

where V_{CELL} is the cell voltage produced and 1.2527 is the voltage equivalent to the lower heating value of hydrogen at 298 K. (This convention is arbitrary, but is widely used.) Voltage increases as load (or current density) decreases. Thus it is possible for overall system efficiency to remain fairly constant as load decreases, the slight decrease in the other efficiencies being compensated by the increase in stack efficiency.

A dominating factor in these calculations is hydrogen utilization. Hydrogen utilization must be decreased with decreasing load to provide sufficient fuel (anode vent gas) heating value to the fuel processor. This relationship is given by the following equations:

$$EF = \left(UH \cdot n_{H_2,P} \cdot LHV_{H_2}\right) \Big/ \left(n_f \cdot LHV_f\right)$$

where EF = fuel processor efficiency

UH = hydrogen utilization

$n_{H_2,P}$ = moles hydrogen produced per hour by the fuel processor

LHV_{H_2} = lower heating value of hydrogen

LHV_f = lower heating value of methanol

n_f = moles per hour of methanol fed to the unit

This equation shows that EF is proportional to UH if other factors are constant. The example that follows shows how the steady-state computer programs are used to calculate system efficiency versus load.

The results of the case studies for the 50kW example are listed in Table II. In this example, which is based in part on heat loss observations with the 5kW integrated system, the heat loss from the system is held constant with load at 27,980 kJ/hr. Although this is the heat lost from both stack and reformer, the majority of this comes from the burner section of the reformer. Also, 2.8 times stoichiometric air to the burner was used in this case study. This high air to anode vent gas ratio was used in the 5kW unit to moderate the combustion-gas temperature in heat-transfer communication with the catalyst. Alternative control schemes are being considered for the 50kW unit.

Table II lists the various calculated values as the current density decreases at constant hydrogen utilization, starting with UH = 80%. Note that the reactor flue-gas temperature drops to an unacceptable level for the fuel processor as the load decreases. The hydrogen utilization must drop as load is decreased until the flue-gas temperature is once again acceptable. Figure 15 is a plot of the overall efficiency versus load.

This type of off-design analysis has now been added to the computer program to lower hydrogen utilization automatically until the reformer heat balance is provided. Work continues in developing this type of fuel cell power-plant analysis.

SECTION II. - CONTINUED

OVERALL SYSTEM DESIGN AND DEVELOPMENT (97064)

The effective utilization of waste heat in absorption chillers requires that the condensing temperature for the working fluid of the chiller be as low as possible, preferably well under 300K. Both the capacity and the Coefficient-of-Performance (C.O.P.) of absorption chillers are strongly dependent on the chiller's condensing temperature. (C.O.P. is defined as the ratio of chilling energy to energy input to the chiller.) It is difficult to generate condensing temperatures below 300K on hot summer days, even with the help of large and expensive cooling towers.

The use of thermal storage based on heat-of-fusion materials is being examined in relation to lowering the average chiller condenser temperature. Such materials are designed to melt and thus absorb heat from the condensing stage of absorption chillers during the day when the outdoor temperature is too high to generate the desired cooling temperatures directly with reasonably sized equipment. The heat-absorbing material can be regenerated at night by letting it freeze and thereby reject heat to the atmosphere. A practical thermal storage material for this application should be inexpensive, have a relatively large latent heat of fusion, and a melting point somewhere between 290K and 293K. A search is being carried out for such a material, and so far a family of proprietary paraffin waxes has been found that comes close to meeting these specifications. Since they are simple petroleum derivatives, these waxes are expected to be fairly inexpensive and non-corrosive. Their heat of fusion is of the order of 40 calories per gram, about half that of ice and among the highest of any ambient temperature melts. The best composition tested so far freezes at 295K, just a few degrees above the usable range. Several new compositions have meanwhile been received and will be tested shortly.

SECTION II. - CONTINUED

A study of how best to utilize waste heat from the fuel cell system is underway. From the work completed so far, it is clear that the amount of waste heat utilized in a year's time critically affects the profitability of owning or leasing an on-site fuel cell system. The size of the fuel cell relative to the site load in turn determines how much of the waste heat can be effectively utilized. For sites with approximately equivalent HVAC load and electrical load, the fuel cell system can be sized at or close to the peak electrical load, especially if some power can be sold back to the electric utility.

For sites with a less favorable ratio of HVAC to electrical load, a connection to the power grid is essential. Such a connection allows the fuel cell system to be sized at less than the peak electrical load, with the power grid supplying the difference. As the fuel cell system is sized down relative to the site peak load, the fuel cell waste heat can be utilized by the site to the greater extent necessary for a positive and attractive cash flow. Most favorable of all are sites with a relatively constant electrical load and a relatively large HVAC load, such as hospitals. Such sites can be profitable even if they are not connected to the power grid.

Sensitivity studies were carried out to assess the effect on the fuel cell system economics of initial system costs, electricity costs, fuel costs, and the relative size of the fuel cell system. These studies indicate that even if the initial cost of the fuel cell system (excluding HVAC) should rise from an estimated $800 per kW (1981 dollars) to $1600 per kW (1981 dollars), there could still be considerable savings and an attractive after-tax return on the differential investment. The results also indicate that a rise in the price of natural gas toward the energy-equivalent price of fuel oil would not by itself destroy the economic advantage of the system, and that a decrease in the constant-dollar price of methanol would

greatly enhance the economics of a methanol-based fuel cell in regions where natural gas is unavailable. Most significantly, an increase in the constant-dollar price of electric power would have a drastically beneficial effect on the economics of either a methanol-based or a natural-gas-based fuel cell system.

TASK IV - STACK SUPPORT (97049)

The purpose of this task, which will continue throughout the contract, is to investigate new materials and component concepts by experimentation and the use of small-stack trials. The criteria for choosing activities under this task will be the possibilities of improved performance or reduced cost, or both. Improvements in, and performances of electrocatalysts, though generated under Engelhard-sponsored Task VI, will be reported under Task IV.

IMPROVED BIPOLAR PLATE PRODUCTION METHODS

Until now the Pfizer process for preparing needled-felt A-elements has consisted of three steps in order of increasing temperature: (1) Carbonization of rayon precursor, (2) Graphitization to increase strength and (3) Chemical vapor deposition (CVD) of additional carbon to 6-8 times original weight. The first two steps have been done while the material was in roll form, while the last has been done after the material was cut into flat sheets. Because Step 2 involves considerable shrinkage, leaving the material in roll form during this step has apparently been responsible for variations in thickness, which have caused a high reject rate.

Trials are now being conducted to combine Steps 2 and 3 into one continuous sequence of increasing temperature. The material is cut and lies flat for this combined step. This is expected to reduce the

SECTION II. - CONTINUED

time required for fabrication as well as provide more uniform thickness of the product. Although testing of this combined step is being conducted in batch lots, similar processing should be achievable in continuous production.

The next step in the production of bipolar ABA plates is bonding of the sandwich with graphite adhesive. During the most recent large-batch run at Pfizer, the adhesive was applied too coarsely, followed by assembly and curing. The results, after assembly and curing, were uneven thickness of the plates, poor electrical conductivity, and difficulty in edge-sealing the plates due to the corrugated configuration of the adhesive layers. Use of these plates in the 5kW stack led to the problems described earlier in Task I.

As the result of follow-up studies between Engelhard and Pfizer, a "green-pressing" step has been adopted between the assembly and curing steps. This pressing is carried out at 70 to 140 kPa (10-20 psi) while the adhesive is still wet. Its effect is to flatten and thin out the adhesive layers in the sandwich. Recent test samples prepared by Pfizer using this modified procedure have been thinner overall and more even in thickness. They also have excellent electrical conductivity (less than 1 mV IR-drop at standard test current, as compared to 15-30 mV drop with the old procedure). No problems with edge-sealing are anticipated. In production now is a replacement set of these improved plates for a rebuild of the 5kW stack.

A new grooving machine has been set up for the machining of constant-depth grooves in finished ABA plates. Since widths of up to 14" can be cut with a single pass, fewer passes will be required to cut a full-sized plate than were required with the old machine. In operation the plate is fed over the grooving wheels by two driven rollers. The grooving wheels are mounted on an arbor located below the work table. The arbor height is adjustable so that the wheels

protrude through the work table to a height corresponding to the required groove depth. Cutter lubrication, cooling and dust suppression are provided by a water spray on the wheels. Modifications might be made later to this machine to permit cutting the plates to size simultaneously with the grooving.

MEASUREMENTS OF ABA PLATE RESISTANCE

An accurate and reliable measurement of plate resistance requires that the contacting surface used to make the measurement be highly conductive and have minimal contact resistance at the plate surface. Thin carbon sheets provide low contact resistance but are not sufficiently conductive to avoid the flow of lateral (planar) currents in the plates; such currents can lead to significant measurement errors. Copper screens are highly conductive, but their tendency to tarnish leads to unreliable electrical contacts which can also generate lateral currents and consequent errors. These problems are avoided with a modified measuring technique using gold-plated copper screens as contacts. The contribution of such screens to the total measured resistance of ABA plates has been found to be well under 1 millivolt, and lateral currents are negligible.

ELECTROLYTE MANAGEMENT

The development and evaluation of an improved electrolyte management system continued this quarter. A new method for storing and distributing electrolyte to individual cells within a fuel cell stack has been under test. This improved electrolyte management system allows for electrolyte replenishment in response to cell demand, without interfering with the normal operation of the electrodes, reactant distribution plates or other cell components.

SECTION II. - CONTINUED

Such an electrolyte management system was demonstrated successfully in a 3-cell stack that has been running for 2000 hours. The anode catalyst in this stack had an original Pt surface-area of 84 m^2/g and was formulated with 45% Teflon (TFE) in the final mix. The corresponding data for the cathode catalyst were 98 m^2/g and 50%. The open-circuit voltage history of this stack is shown in Figure 16 and the load voltage in Figure 17. It is planned to continue this test for at least another 1000 hours.

The peak open-circuit voltage shown was 900 mV/cell and the average open-circuit voltage was 887 mV/cell (Figure 16). After 1300 hours the electrolyte replenishment was interrupted for 350 hours. This planned interruption caused a decrease in the stack performance, reducing the average open-circuit voltage to 870 mV. When the electrolyte replenishment was resumed the open-circuit voltage recovered to 877 mV/cell.

Under standard load (161 mA/cm^2) a peak voltage of 643 mV/cell was obtained and an average voltage, prior to the interruption, of 637 mV/cell. The interruption in the electrolyte replenishment caused a decrease in the average to 620 mV, which recovered to 625 mV upon resumption of electrolyte feed.

Results of stack tests of an earlier version of the electrolyte management system were summarized in the August, 1981 Monthly Technical Progress Narrative, pp. 8-9.

CORROSION TESTING OF CATALYST CARBON SUPPORTS

The improved corrosion resistance of a stabilized carbon support material (heat-treated) is shown in Figure 18. An electrocatalyst using this stabilized carbon support showed significantly

SECTION II. - CONTINUED

lower corrosion current than the base-line type at 1.0 volt (vs. reversible hydrogen electrode) and 204°C. The test at 1.0 volt has been used in this laboratory in the past as a basis for comparison only; it is more severe than the actual conditions the material would encounter.

EVALUATION OF PLATINUM RECRYSTALLIZATION

The Pt surface-area losses for a developmental electrocatalyst during cell operation were determined using cyclic voltammetry. The catalyst was of the stabilized-Pt/stabilized-support type (#11175-33-2). Voltammograms before and after 6000 hours of service are shown in Figure 19. The Pt surface-area loss is clearly indicated in the reduction of the area under the hydrogen adsorption peaks. (The initial sharp peak on the oxidizing cycle is not due to adsorbed hydrogen.) The loss as a function of time is plotted in Figure 20. The catalyst maintained a surface-area of 45 m^2/g Pt after the 6000-hour period, or slightly less than half its original value.

Another developmental electrocatalyst of the stabilized-Pt/stabilized-support type (#11445-48) showed improved resistance to platinum sintering when tested in an aging cell against a base-line catalyst. Figure 21 shows the Pt surface-areas of both these catalysts as a function of time at 0.7V (vs. reversible hydrogen electrode) and 477 K (204°C). After 1000 hours of testing the developmental catalyst maintained a surface-area of 45 m^2/g Pt, whereas the base-line catalyst showed a surface-area of only 15 m^2/g Pt.

TASK V - FUEL PROCESSING SUPPORT (97050)

The intent of this task is to provide background data and information to support the design and construction of an optimized 50 kW fuel processor under Task III. This support function will

SECTION II. - CONTINUED

continue throughout most of the period of the contract. Most of the effort of this task will be devoted to screening and longevity testing of catalyst for methanol/steam reforming.

Two commercially available catalysts have been evaluated in the sub-scale unit to select a preferred catalyst for the OS/IES fuel processor. The samples are being evaluated in aging runs at space-velocities about double that to be used in the commercial unit. This accelerates the aging if feedstock impurities are a factor in activity decline. Also, it provides conversions below 100% such that rate constants can be calculated and declining activity observed.

The two oxide catalysts, both as 1/8" x 1/8" tablets (3.2mm D x 3.2mm L), have the following approximate compositions:

UCI Catalyst No.	Bulk Density, g/ml	Composition, Wt. % Cu	Cr	Zn	Al_2O_3
T2107RS	1.088	27.5	1.0	11.6	29.9
C70-2RS	1.548	-	22	55	-

In the aging test, the methanol/water mix containing 1.3 moles H_2O per mole of water was fed from a precise metering pump (Ruska) at 16.3 ml per hour over 10 ml of catalyst logarithmically diluted with alumina to produce a nearly isothermal profile. Thus the liquid-hourly-space-velocity was the same for both catalysts; i.e., ml of mix per hour per ml of catalyst was constant.

The test run on T2107RS was reported in the July, 1981 Quarterly Report, p. 12. The performance was stable with commercial grade methanol but declined with a mixture containing 800 vppm ethanol in the methanol. Also, the activity did not recover upon

SECTION II. - CONTINUED

return to the original mixture. The used catalyst was analyzed for carbon accumulation and compared to the virgin catalyst. Such catalysts contain carbon on the virgin sample since graphite is used as a lubricant during manufacture. The results are listed below:

T2107RS Virgin	2.25% Carbon
T2107RS Used	3.13% "

Repeat analysis on both samples gave identical results to two decimal places. Although this is a small increase in carbon, the metal surface-areas of used copper catalysts are small due to copper crystallite growth and could be rendered partially inactive by even this small amount of carbon.

The results to date for C70-2RS are listed in Table III and shown in Figure 22. This catalyst is very stable even with an operating temperature of 643 K (370°C), which is about 100°C above that used with T2107RS. The sample appears capable of tolerating 800 vppm ethanol (typical value for "crude" methanol); good recovery is noted after returning to the original feed. The temperature has since been increased to 673K (400°C) and nearly 100% conversion is observed with a feedstock spiked with 800 vppm ethanol. The aging run is still in progress.

In summary, the Zn/Cr type of catalyst, although initially less active than the Zn/Cu type, has better retention of activity and better tolerance to high temperatures and ethanol poisoning.

TASK VI - IMPROVED ELECTROCATALYSTS (97039)

Developmental electrocatalyst formulations are being prepared under Engelhard sponsorship. These are provided to the main program, and results are reported under Task IV.

SECTION III. CURRENT PROBLEMS

The difficulties with recent Pfizer-produced ABA bipolar plates have been previously described. The changes in procedure intended to bring the plates up to specification are outlined in the present report under Section II, Task IV. From tests on small samples made by the modified procedure it is clear that the problems of excessive thickness and poor electrical conductivity have been solved. Pfizer will soon produce a run of plates by the modified procedure to be used for a rebuild of the 5kW stack. From the appearance of the small test samples it is believed that there will no longer be a problem with edge-sealing. A definite conclusion on this point, however, must await an edge-seal check on some of the stack plates now in production.

SECTION IV. WORK PLANNED

TASK I

- Pfizer to produce ABA plates by modified procedure for rebuild of the 5kW stack.

TASK II

- A. D. Little, Inc. to complete economic feasibility study for OS/IES site in a retail store and recommend 3-4 building types for further study.

TASK III

- Variable-stack test fixture for one to twenty-four full-size cells to be built.

TASK IV

- Continue evaluation of acid replenishment system.

TASK V

- Continue ethanol-poisoning tolerance test on C70-2RS methanol/steam reforming catalyst.

SECTION V. FINANCIAL MANAGEMENT ANALYSIS

TASK I - 5kW POWER SYSTEM DEVELOPMENT

Additional expenditures were accumulated on Task I during October. These were related partly to limited integrated system testing and partly due to late invoicing of materials. Costs are somewhat above budget, primarily due to larger than anticipated materials expenditures. Labor hours are essentially at the level projected for this task.

TASK II - ON-SITE SYSTEM APPLICATION ANALYSIS

Expenditures by Arthur D. Little, Inc. during October were at the projected rate. Cumulative costs are below projections, however, due to a lag in invoicing and relatively low expenditures in earlier months.

TASK III - ON-SITE SYSTEM DEVELOPMENT

1. Large Stack Development

Expenditures on this sub-task were high in October as effort on scaled-up stack components was intensifying. Total spending to date, however, remains below projections.

2. Large Fuel Processor Development

Labor hours and costs were somewhat above the projected rate in October. Cumulative hours and costs, however, are still below the budget through October.

SECTION V. - CONTINUED

3. System Analysis

The apparent costs for this sub-task during October were about twice the normal amount because of previous invoicing being charged. The total expenditures at Physical Sciences Inc. through October are essentially at the projected levels.

4. System Integration

A minor amount of work was performed on this sub-task during October. Earlier effort on the HVAC sub-system had accelerated the schedule. Total costs to date are at the original projections.

TASK IV - STACK SUPPORT

Manpower and costs were at the projected rate during October, even though the Pfizer subcontract for bipolar plate scale-up and cost reduction has not yet begun. Total hours and costs through October are at about 75% of anticipated levels.

TASK V - FUEL PROCESSING SUPPORT

Sub-scale tests involving qualification of large batches of catalyst are continuing. Manpower requirements for these activities have been reduced from anticipated levels. Total expenditures, therefore, remain at roughly half of those projected.

TASK VI - IMPROVED ELECTROCATALYSTS

The development of advanced anode and cathode catalysts is proceeding under Engelhard sponsorship. Evaluation of these catalysts is accomplished under Task IV.

SECTION V. - CONTINUED

TASK VII - MANAGEMENT AND DOCUMENTATION

Expenditures in the management and documentation area are proceeding substantially according to plan.

ENGELHARD

TABLE I

REASONS FOR TURBOCHARGING

REDUCES STACK AREA

IMPROVES PERFORMANCE BY:

INCREASING OPERATING TEMPERATURE

INCREASING PARTIAL PRESSURES OF REACTANTS

IMPROVES POWERPLANT EFFICIENCY

ENABLES HIGH HYDROGEN UTILIZATIONS

CUT WASTE HEAT LOSS

ELIMINATES PARASITIC LOSS OF BLOWER

REDUCES POWERPLANT COST

REDUCES FUEL PROCESSOR SIZE

REDUCES PLUMBING SIZE

CUTS WATER RECOVERY SYSTEM SIZE

CUTS STACK SIZE

IMPROVES POWERPLANT LIFE

REDUCES ELECTROLYTE LOSS

TABLE II

SUMMARY OF RESULTS FROM THE CASE STUDIES FOR 50kW SYSTEM

(Heat Loss from Reformer = 27,980 kJ/hr)

UH	ASF	V	PN	PG	EO	EF	EM	EI	ES	REACTOR FLUE GAS ENTRANCE TEMP.,K
0.8	150	0.615	45.5	51.6	35.6	82.4	97.9	90	49.1	816
0.8	125	0.631	38.9	44.2	36.6	82.4	98.0	90	50.4	779 *
0.75	150	0.616	45.6	51.7	33.5	77.2	97.9	90	49.2	895
0.75	125	0.632	39.0	44.3	34.4	77.2	97.9	90	50.5	866
0.75	112.5	0.640	35.6	40.3	34.8	77.2	98.0	90	51.1	846
0.75	90	0.655	28.1	33.0	34.3	77.2	97.8	87	52.3	797
0.75	75	0.664	23.2	27.9	34.0	77.2	97.7	85	53.0	747 *
0.70	150	0.617	45.7	51.9	31.3	72.1	97.8	90	49.3	955
0.70	125	0.633	39.1	44.3	32.1	72.1	97.9	90	50.6	931
0.70	112.5	0.641	35.6	40.4	32.5	72.1	97.9	90	51.2	916
0.70	90	0.656	28.1	33.0	32.1	72.1	97.8	87	52.3	876
0.70	75	0.665	23.2	27.9	31.8	72.1	97.7	85	53.1	835
0.70	60	0.675	18.3	22.7	31.4	72.1	97.4	83	53.8	774 *
0.70	45	0.684	13.5	17.2	30.9	72.1	97.0	81	54.6	717 *

UH = HYDROGEN UTILIZATION
ASF = CURRENT DENSITY, 100% LOAD = 161 mA/cm^2
V = CELL VOLTAGE
PN = NET POWER, KW
PG = GROSS POWER, KW

EO = OVERALL EFFICIENCY = EF* EM*ES*EI, %
EF = FUEL PROCESSOR EFFICIENCY, %
EM = MECHANICAL EFFICIENCY, %
EI = INVERTER EFFICIENCY, %
ES = STACK EFFICIENCY = V/1.2529 x 100, %

* Below the lower reactor temperature limit of 780K.

Burner Enrichment = 2.8 times stoichiometric for all calculations.

ENGELHARD

Table III

Experimental Data

Methanol/Steam Reforming Catalyst Test

Water/Methanol Molar Feed Ratio = 1.3

Catalyst: UCI C70-2RS Zinc/Chromium Oxide
1/8" x 1/8" Pellets
10 cc in 90 cc alpha alumina, mixed logarithmically

Hours on Stream	Avg. Bed Temp., K	Exit Bed Temp., K	% CO	WHSV **	% MeOH Conversion	Kinetic Rate Constant, k*
			Runs with Pure Methanol/Water			
23	623.1	625.0	0.65	0.6	77.03	0.067
71	641.3	646.5	1.32	0.6	93.17	0.166
168	642.2	635.0	1.22	0.6	93.15	0.166
242	641.6	641.8	1.14	0.6	91.77	0.149
336	641.1	645.8	1.06	0.6	91.14	0.142
487	640.6	644.1	1.15	0.6	83.55	0.091
	Shut down for two weeks - equipment problems (controller).					
529	643.3	625.2	1.04	0.6	81.35	0.081
649	642.0	641.0	1.00	0.6	79.01	0.073
700	644.3	644.5	1.42	0.60	84.64	0.096
771	642.5	633.0	1.29	0.60	81.60	0.082
842	643.5	642.6	1.18	0.60	83.71	0.091
961	644.0	638.0	1.14	0.60	86.6	0.107
1082	642.0	648.0	1.10	0.61	84.86	0.097
1144	643.0	642.0	1.04	0.60	84.6	0.096
			Add Ethanol (800 ppm)			
1239	642.2	641.8	0.95	0.60	73.24	0.067
1311	641.1	642.9	0.91	0.60	74.08	0.059
1408	641.9	641.8	1.02	0.60	73.28	0.057
1479	643.2	642.9	1.05	0.60	79.45	0.074
			Back to Pure Methanol/Water			
1575	640.2	635.0	0.85	0.60	84.89	0.097
1646	645.1	632.4	1.02	0.60	88.5	0.119
1741	639.6	642.6	1.10	0.60	82.86	0.087
1812	642.0	641.3	1.15	0.60	87.22	0.110
1920	644.2	639.8	1.01	0.60	88.53	0.119
			Raise Temperature - Add Ethanol (800 ppm)			
1968	674.2	382.2	2.41	0.60	99.45	0.438

* $k = \left[\frac{\text{kg MeOH Feed}}{\text{kg reduced Catalyst x hr}}\right] \cdot \left[\frac{\text{m}^3 \text{ Feed}}{\text{kg moles feed}}\right]$

** Weight-hourly Space-Velocity $\left[\frac{\text{kg MeOH Feed}}{\text{kg reduced catalyst x hr}}\right]$

ENGELHARD

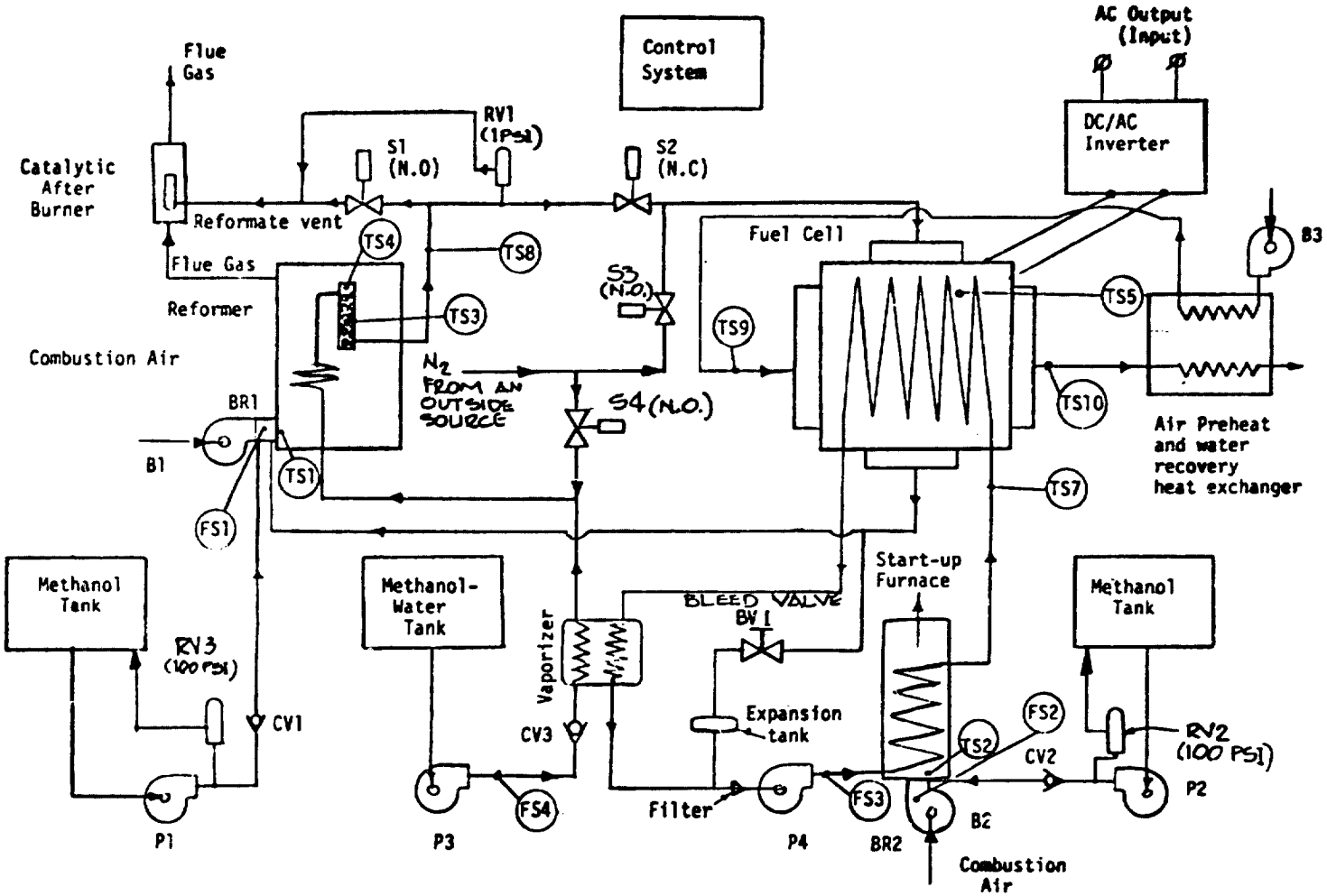

FIGURE 1 5kW INTEGRATED SYSTEM SCHEMATIC

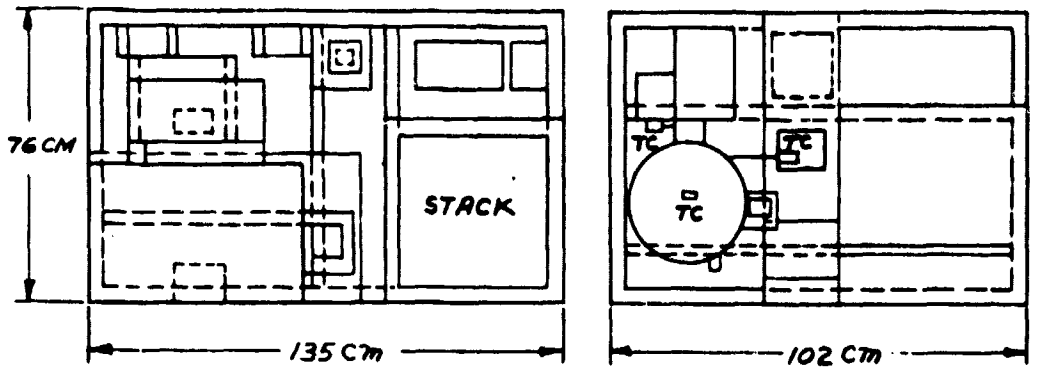

TOP VIEW

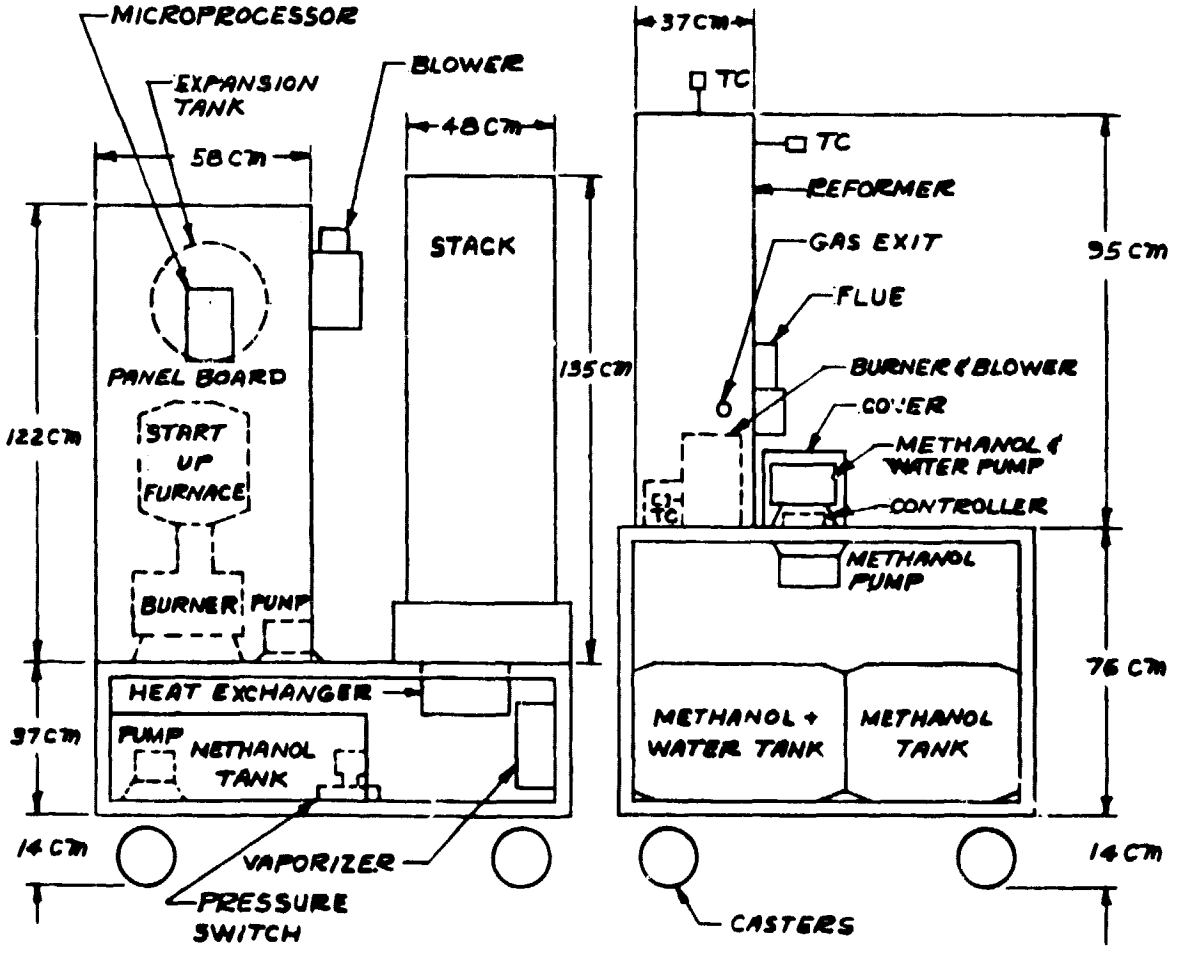

FRONT VIEW

FIGURE 2 LAYOUT OF 5kW INTEGRATED SYSTEM ON TWO MOVEABLE CARTS

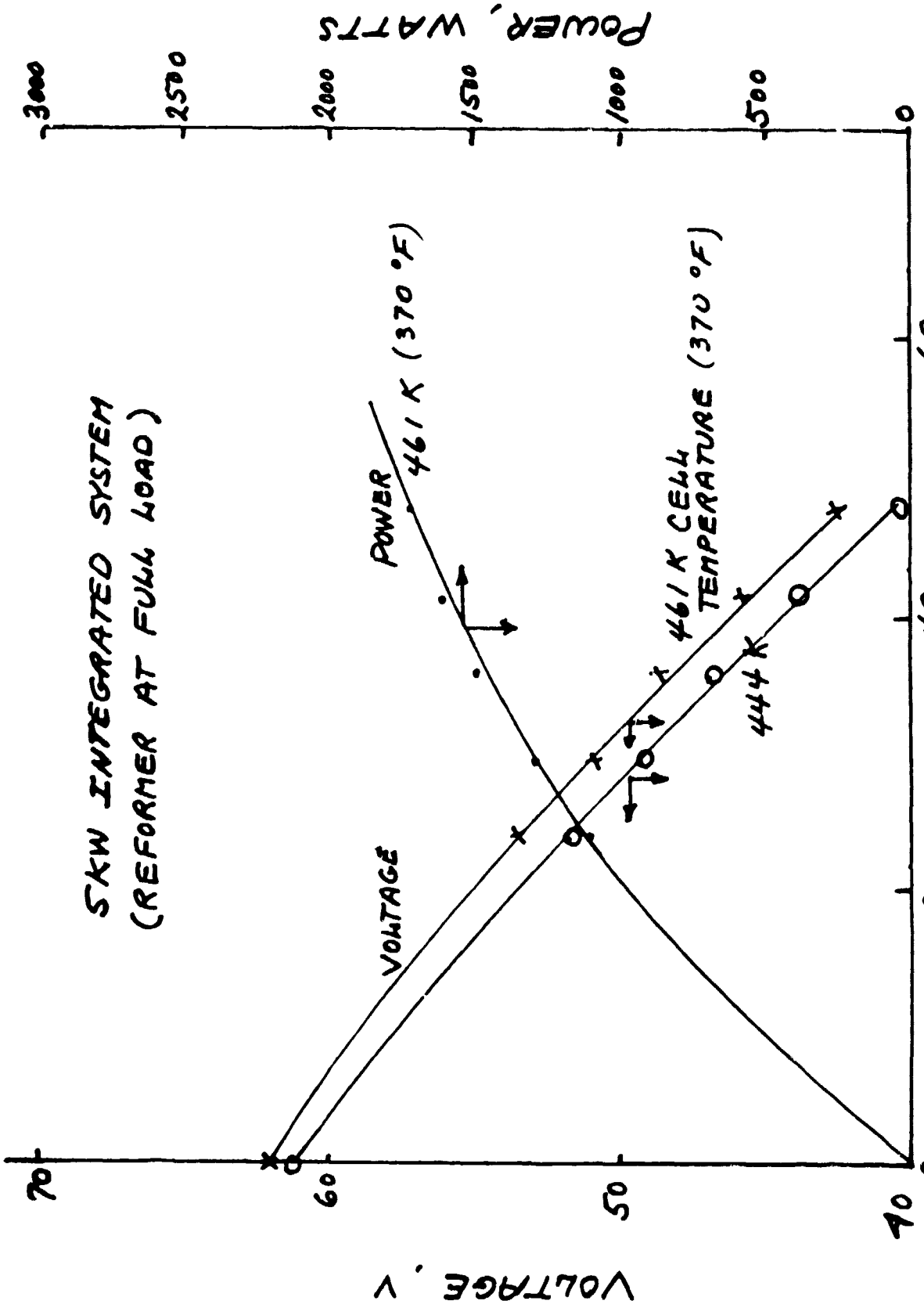

FIGURE 3 EFFECT OF CELL TEMPERATURE ON PERFORMANCE

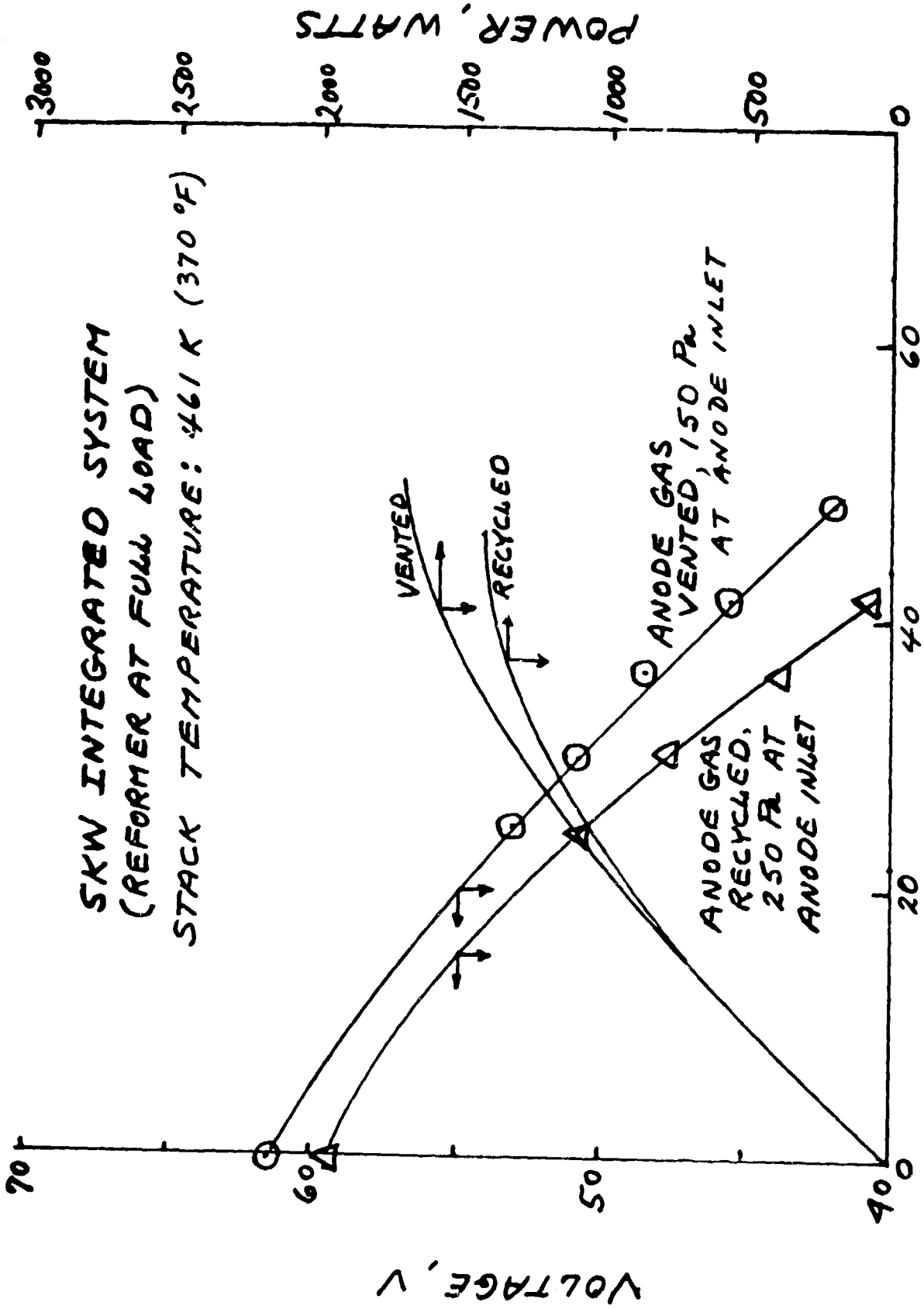

FIGURE 4 EFFECT OF ANODE VENT GAS RECYCLE ON PERFORMANCE

ENGELHARD

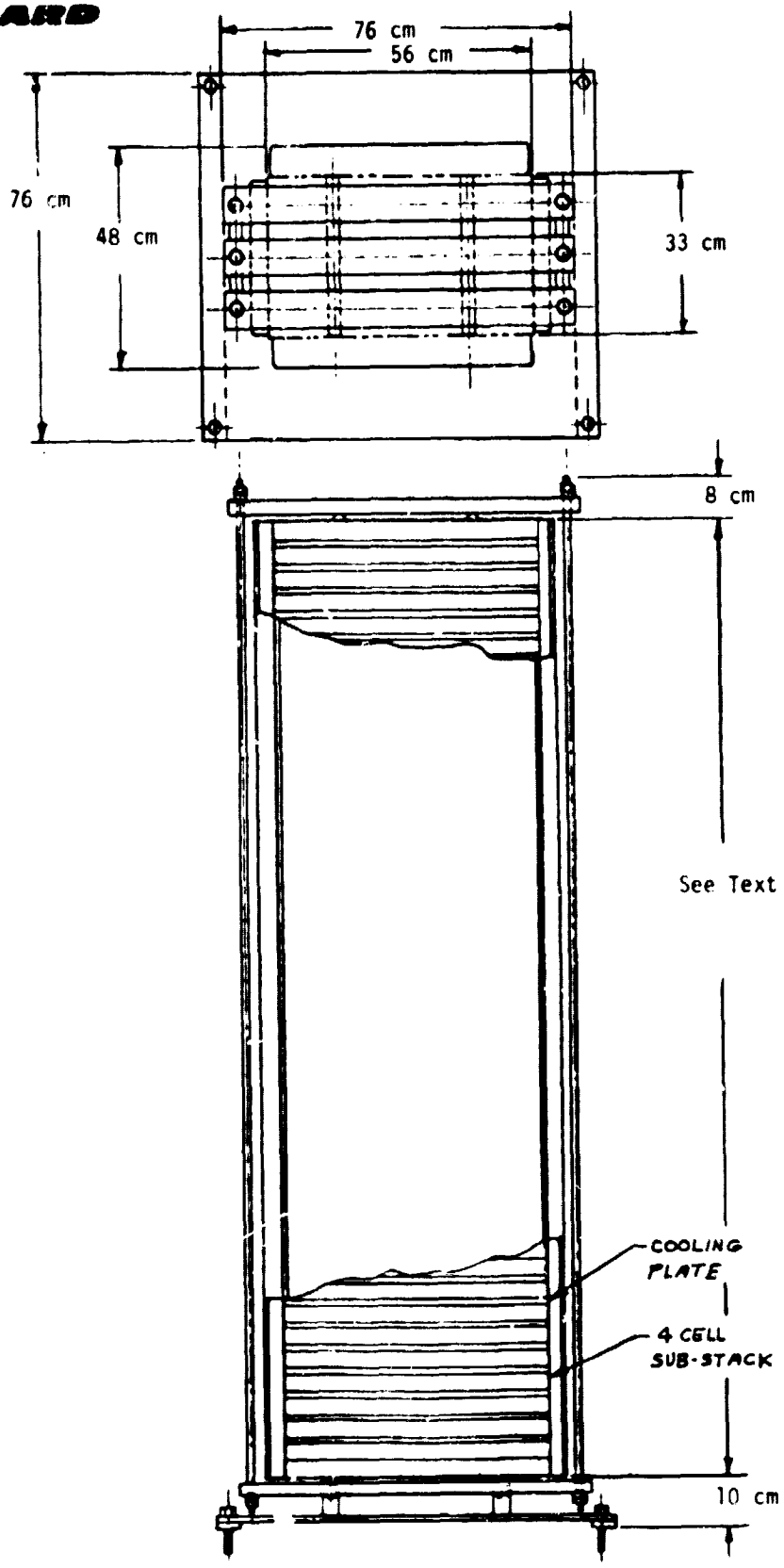

FIGURE 5 SKETCH OF 25kW STACK

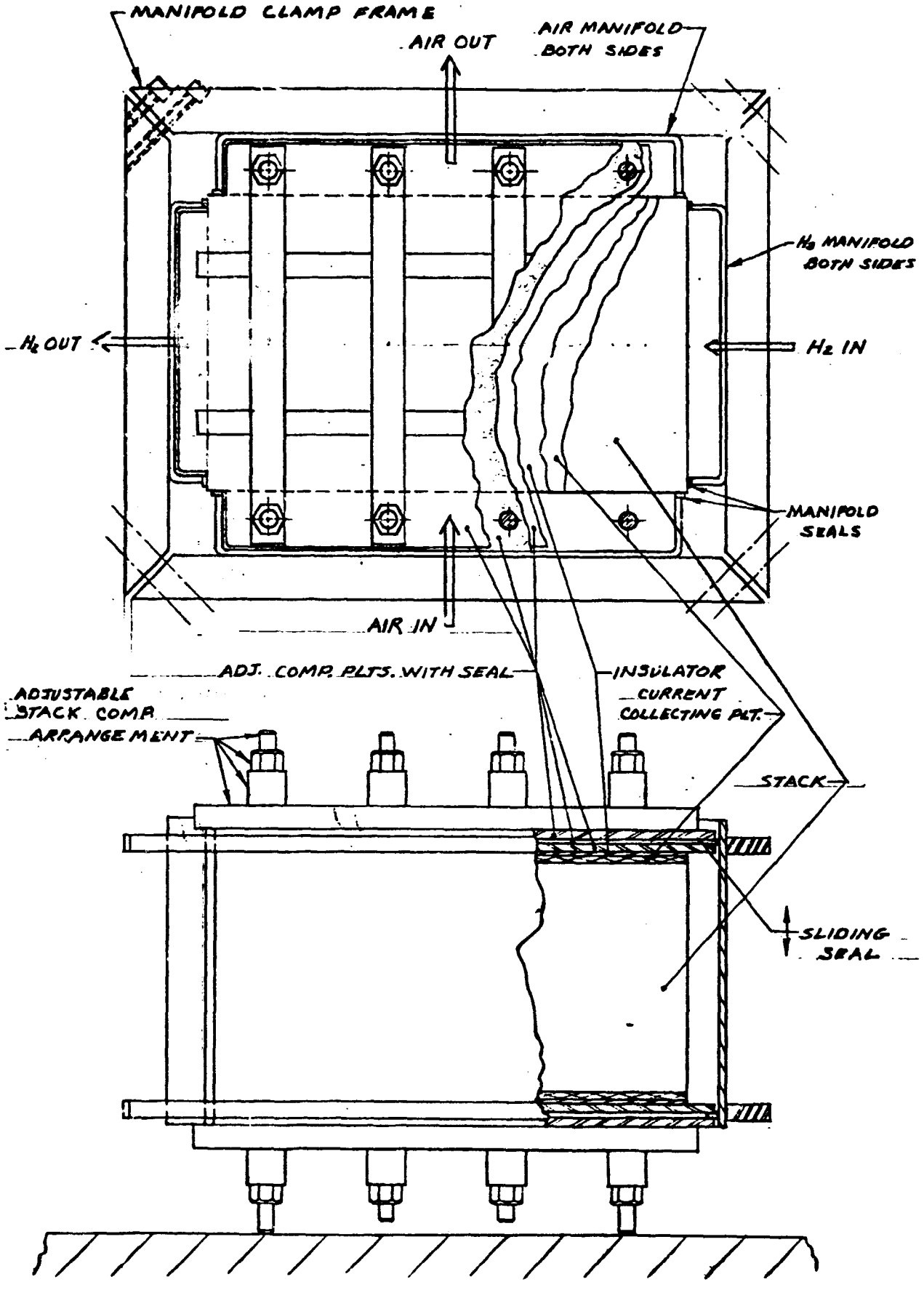

FIGURE 6 VARIABLE STACK TEST FIXTURE FOR ONE TO TWENTY-FOUR FULL-SIZE CELLS

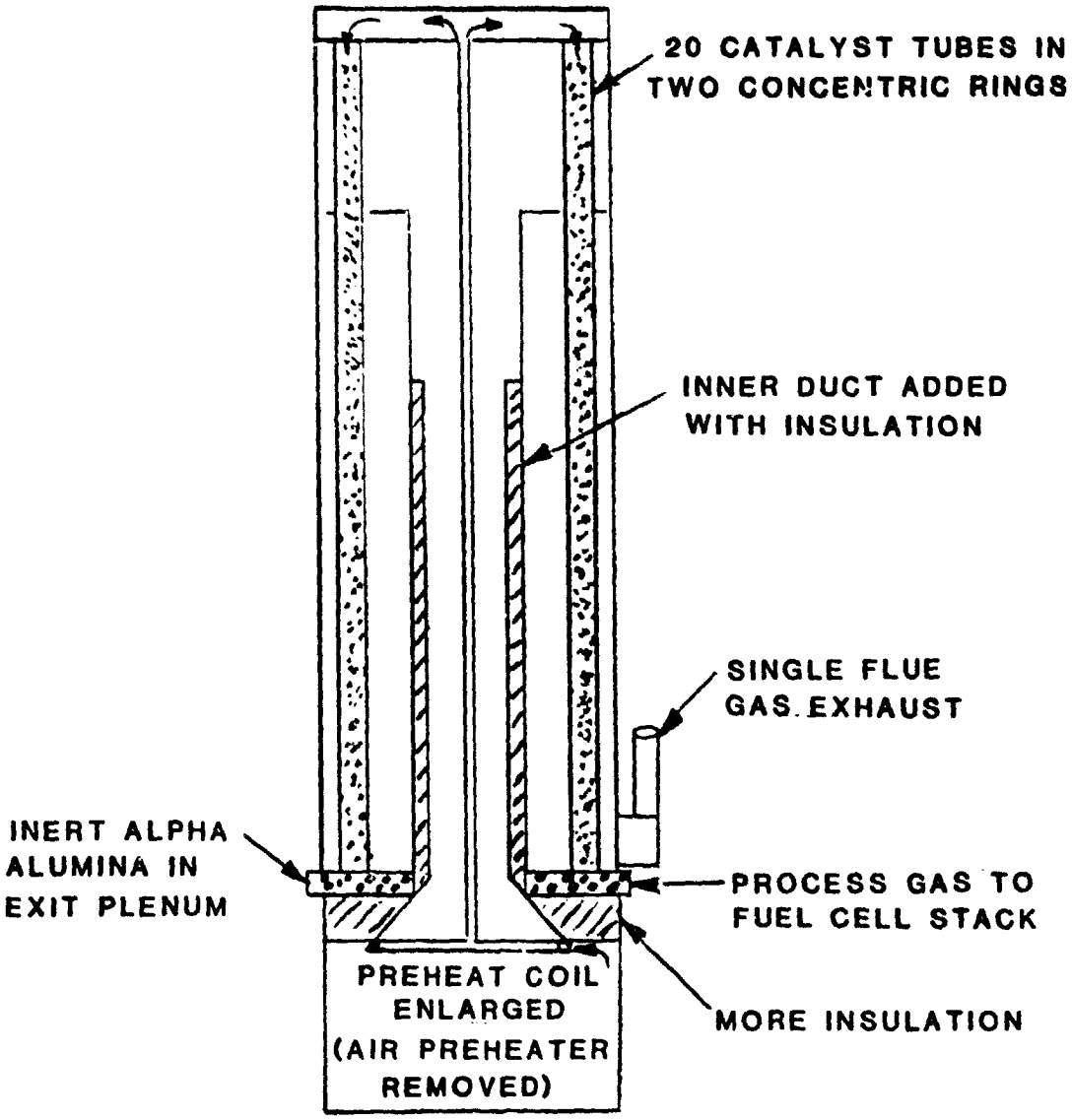

FIGURE 7 REVISION TO 5kW REFORMER

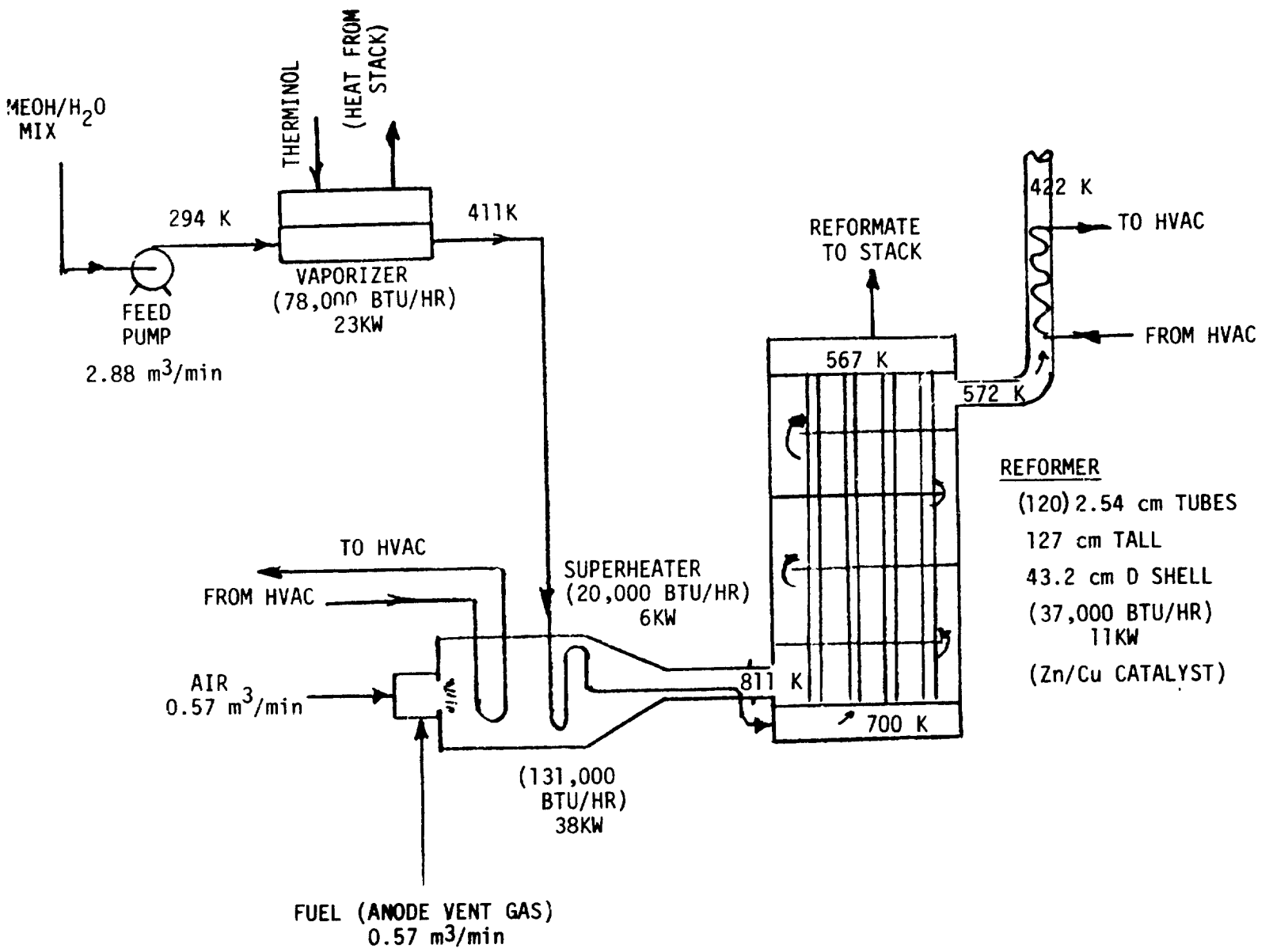

FIGURE 8 50 kW REFORMER FOR OS/IES OPERATING AT 80% HYDROGEN UTILIZATION

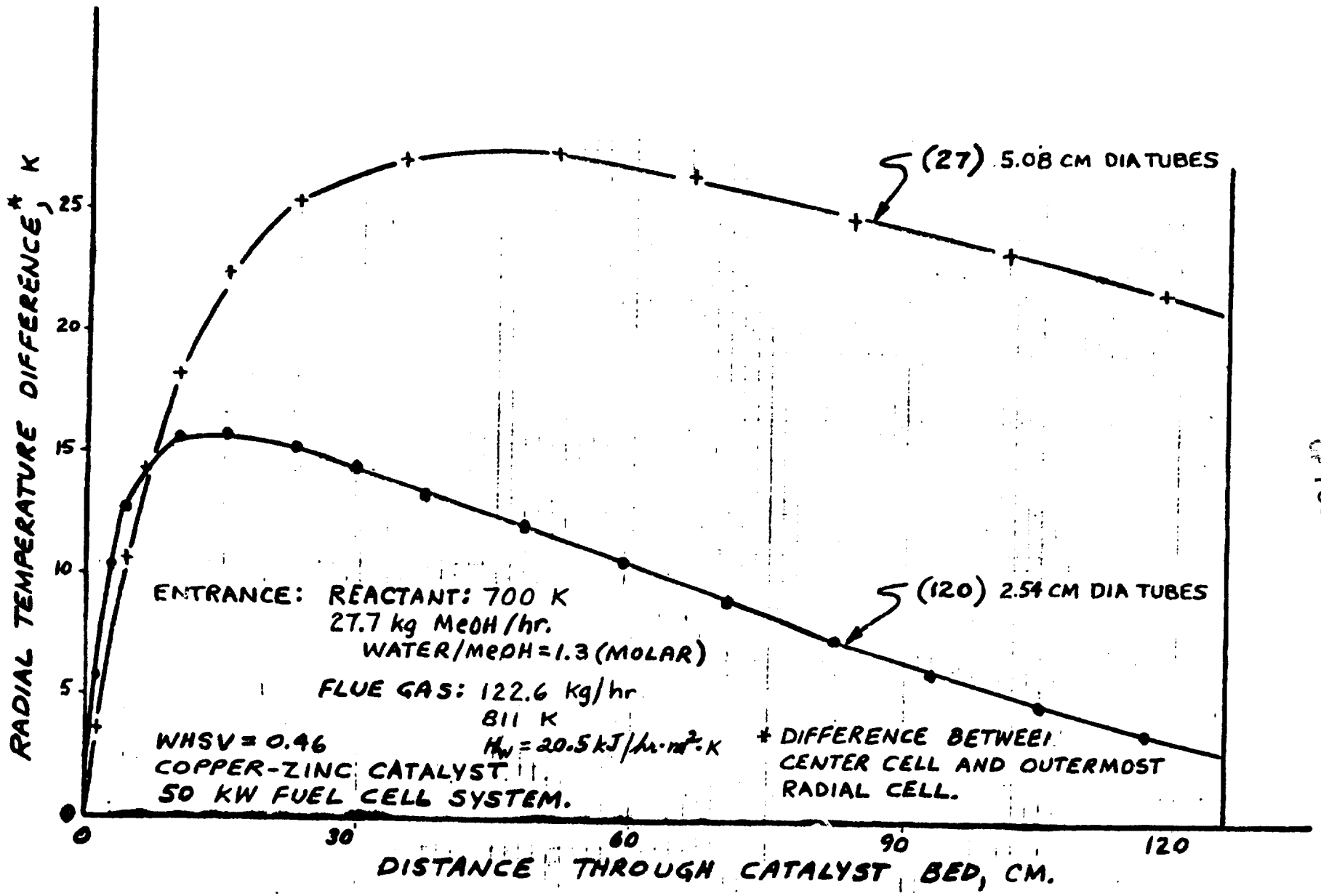

FIGURE 9 RADIAL TEMPERATURE DIFFERENCE PROFILES IN METHANOL/STEAM REFORMER - PREDICTION BY TWO-DIMENSIONAL MATH MODEL

ENGELHARD

ORIGINAL PAGE IS
OF POOR QUALITY

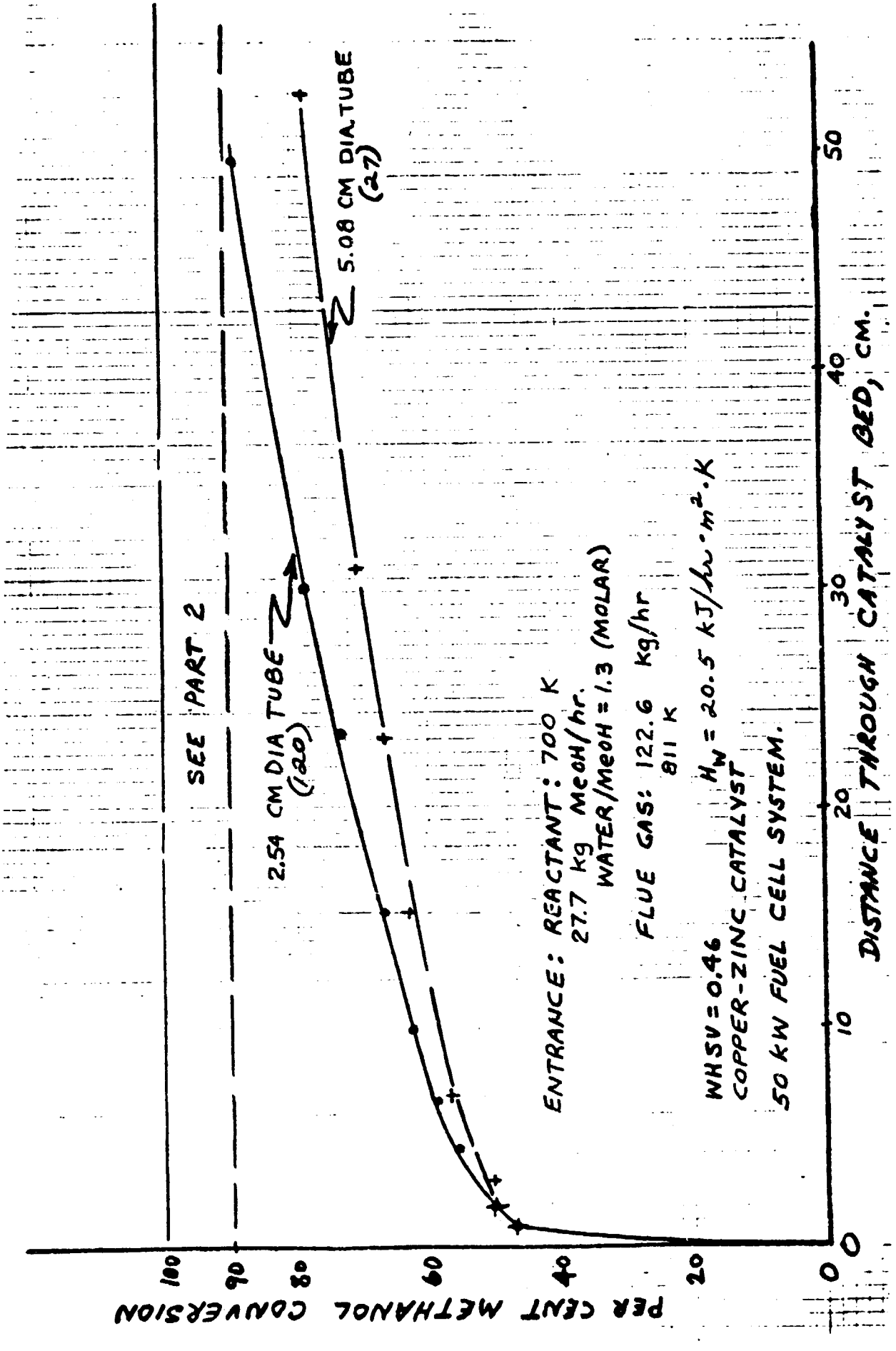

FIGURE 10 CONVERSION PROFILE IN METHANOL/STEAM REFORMER - PREDICTION BY TWO-DIMENSIONAL MATH MODEL (PART 1)

ENGELHARD

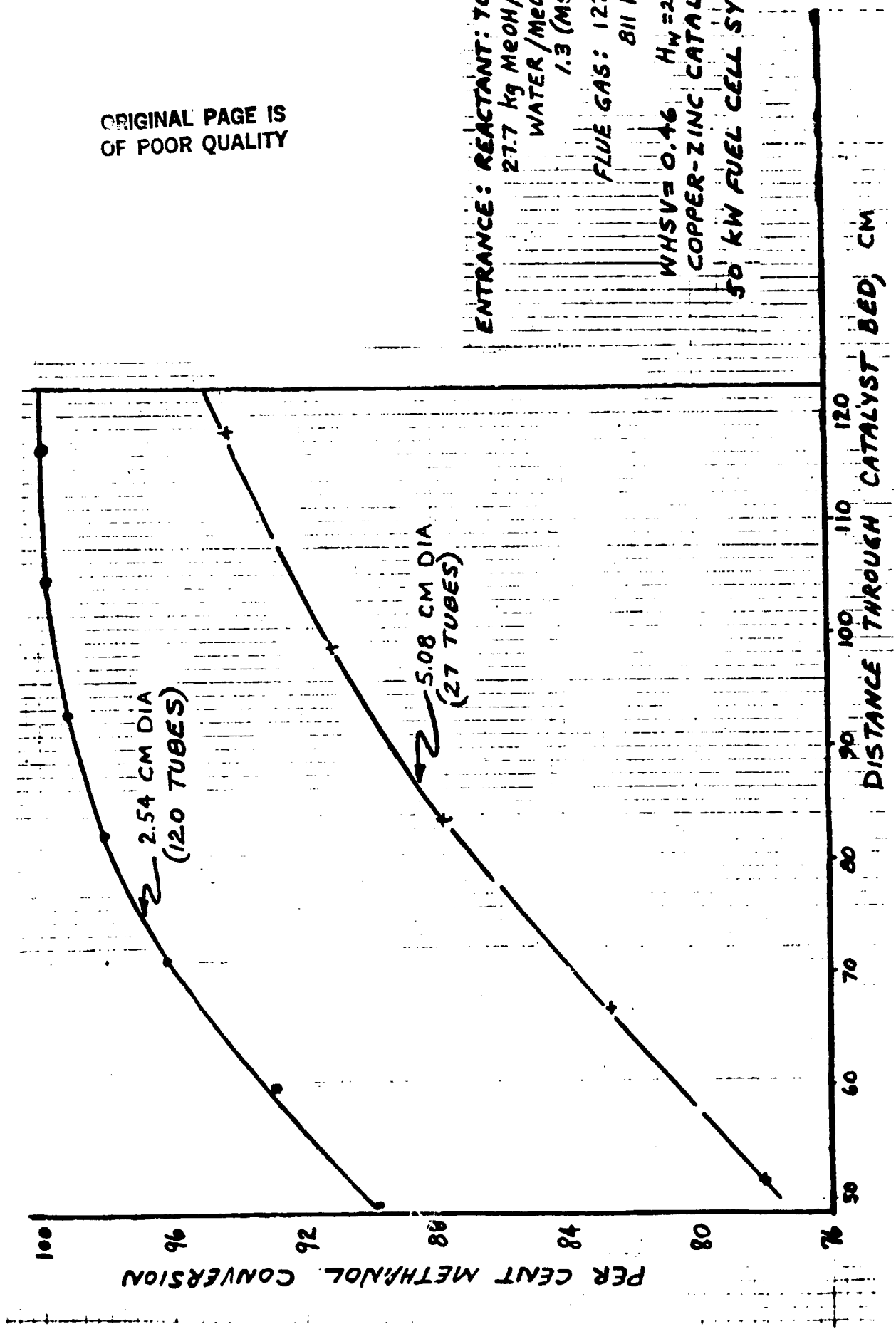

FIGURE 11 CONVERSION PROFILE IN METHANOL/STEAM REFORMER - PREDICTION BY TWO-DIMENSIONAL MATH MODEL (PART 2)

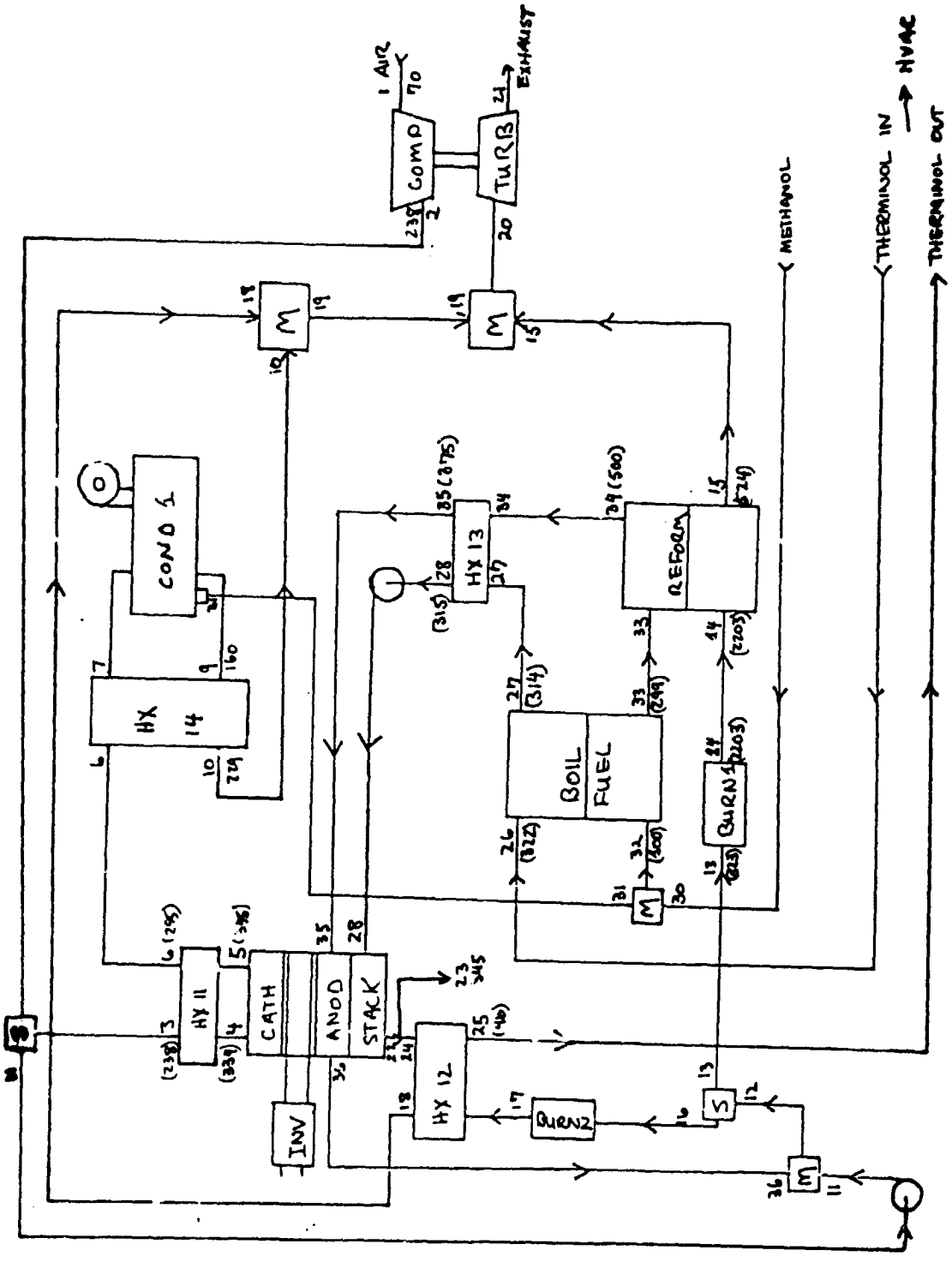

FIGURE 12 SCHEMATIC OF A PRESSURIZED FUEL CELL POWER PLANT

TURBOCHARGING PRODUCES A 20% INCREASE IN OVERALL PLANT EFFICIENCY

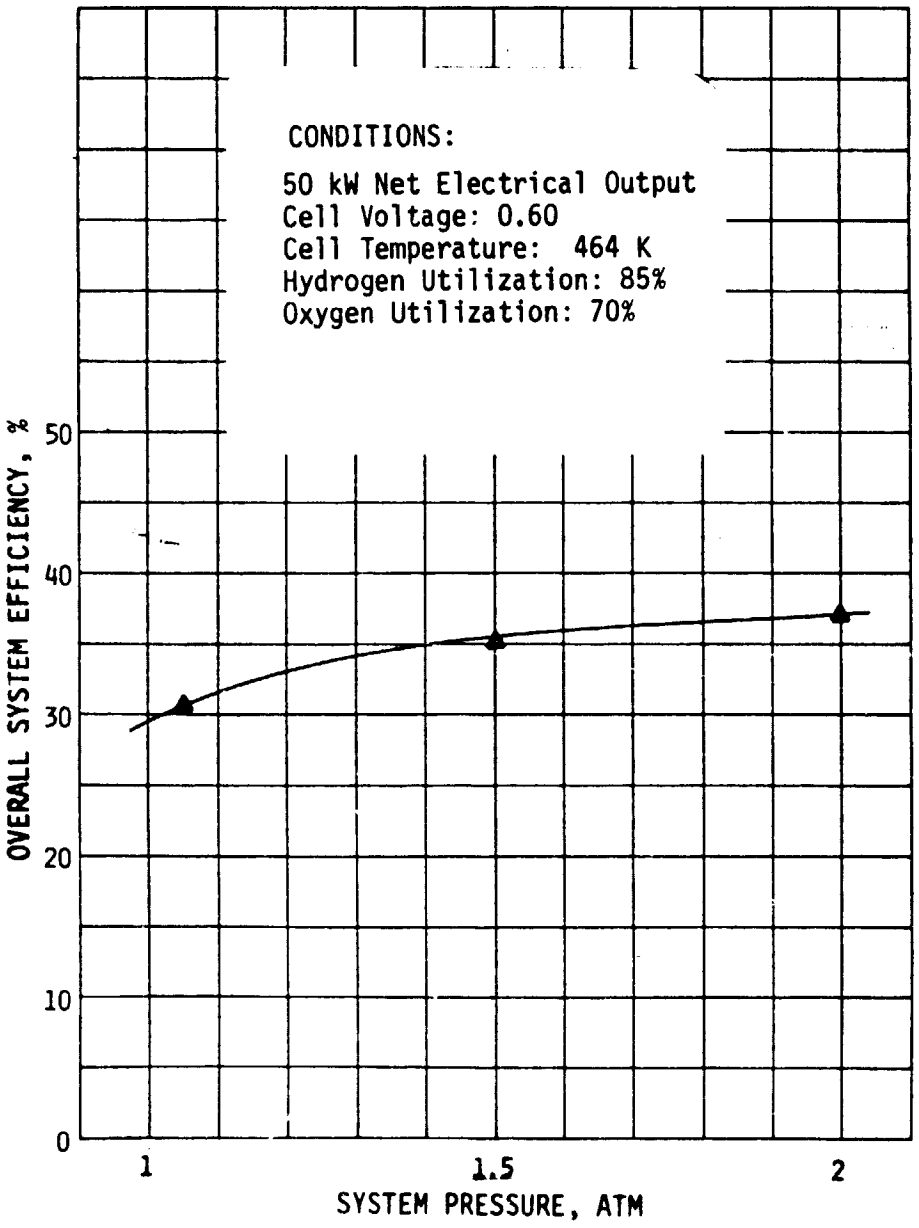

FIGURE 13 OVERALL PLANT EFFICIENCY VERSUS PRESSURE

TURBOCHARGING THE PLANT RESULTS IN A 40% REDUCTION IN STACK SIZE

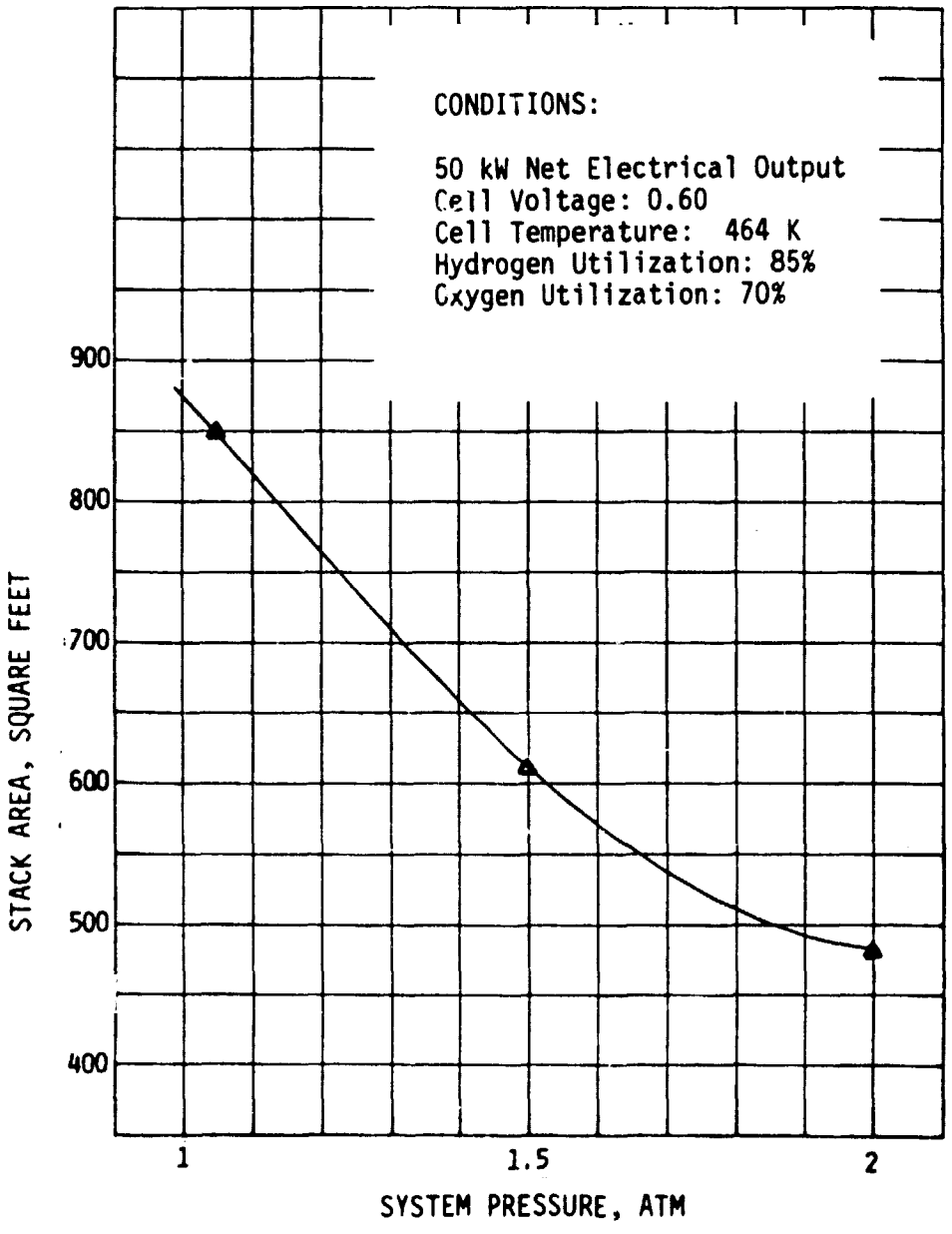

FIGURE 14 STACK AREA VERSUS PRESSURE

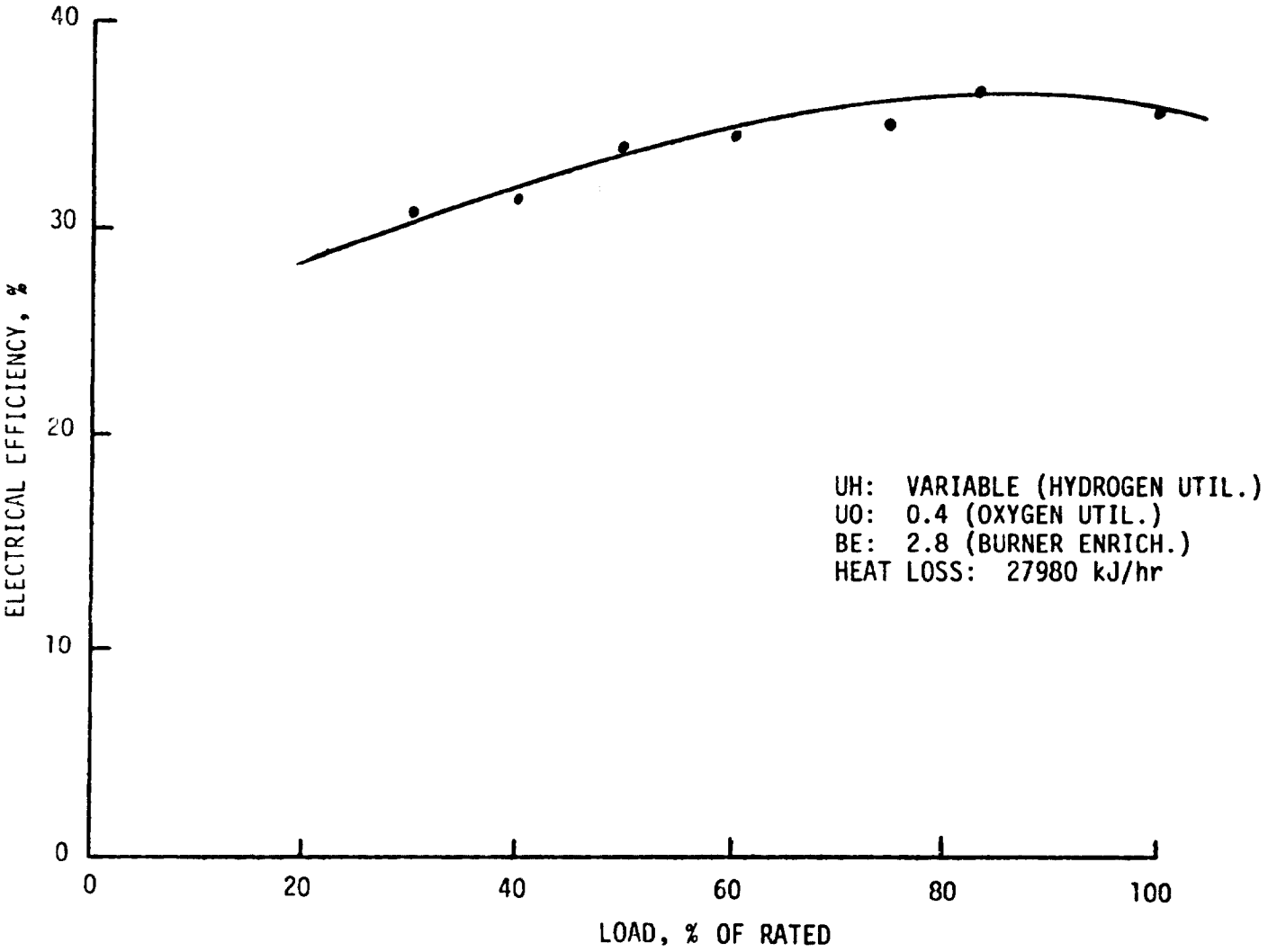

FIGURE 15 OVERALL ELECTRICAL EFFICIENCY VERSUS LOAD

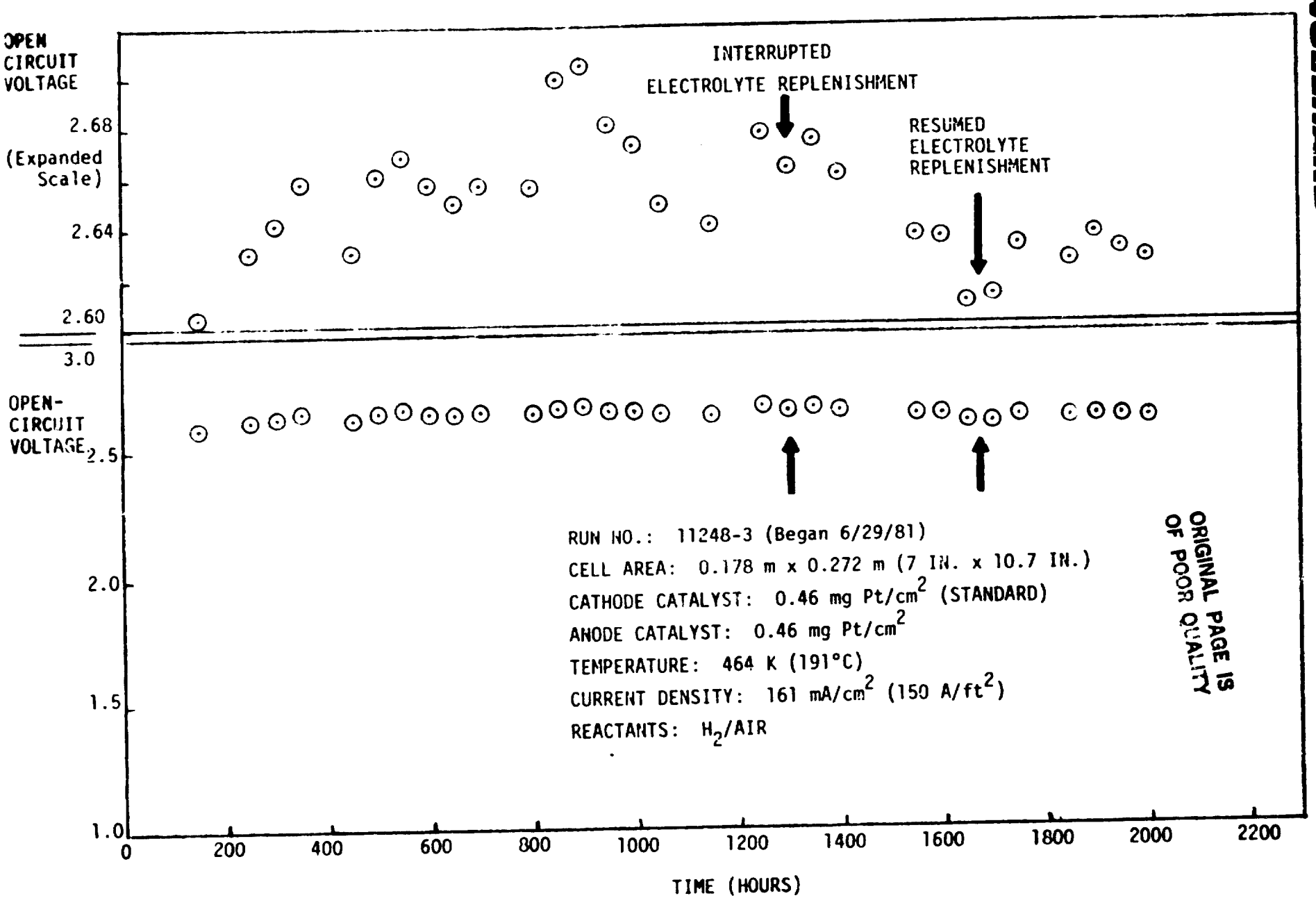

FIGURE 16 OPEN-CIRCUIT STABILITY OF 3-CELL STACK UTILIZING A NOVEL ELECTROLYTE REPLENISHMENT SYSTEM

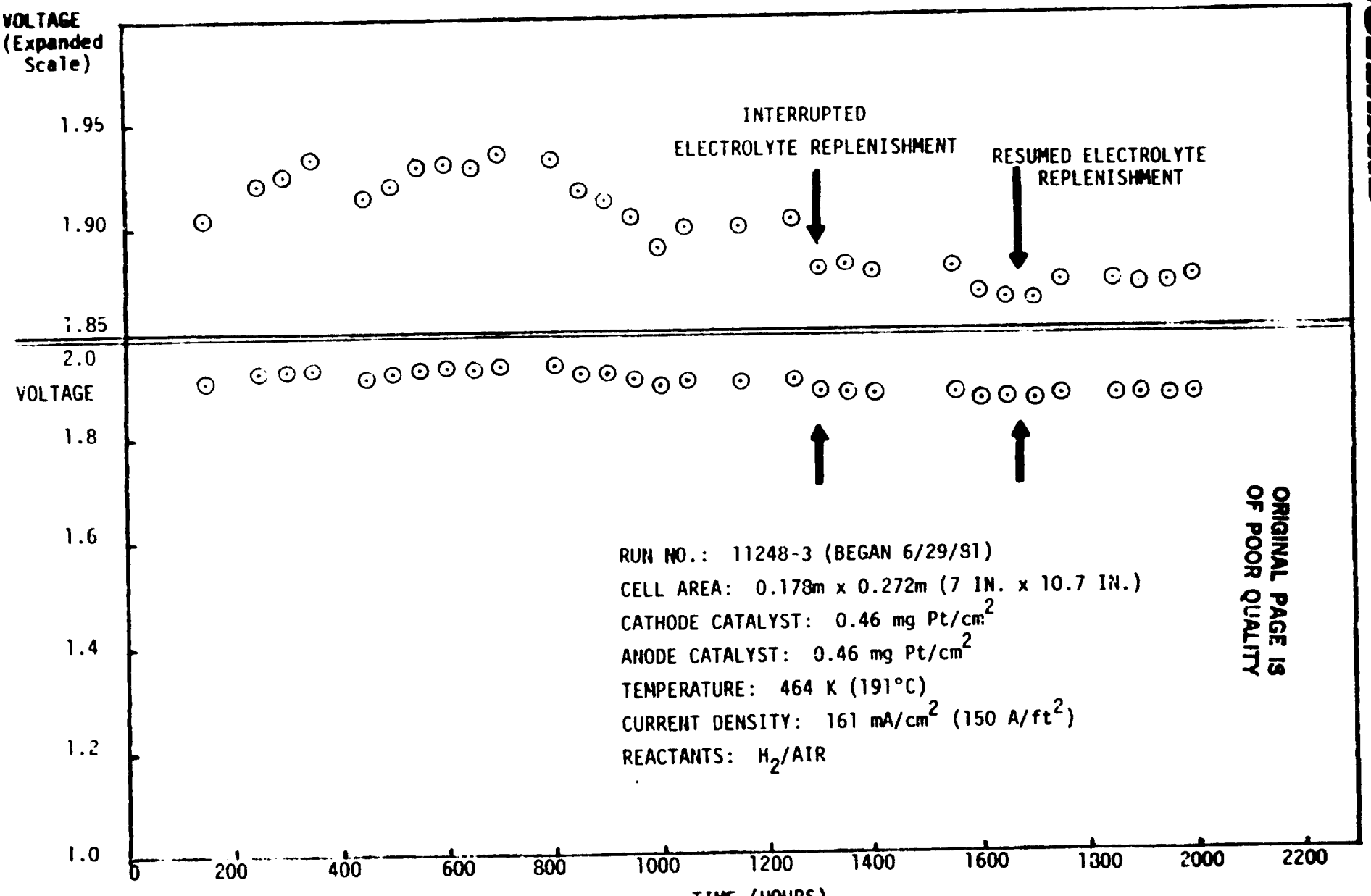

FIGURE 17 PERFORMANCE STABILITY OF 3-CELL STACK UTILIZING A NOVEL ELECTROLYTE REPLENISHMENT SYSTEM

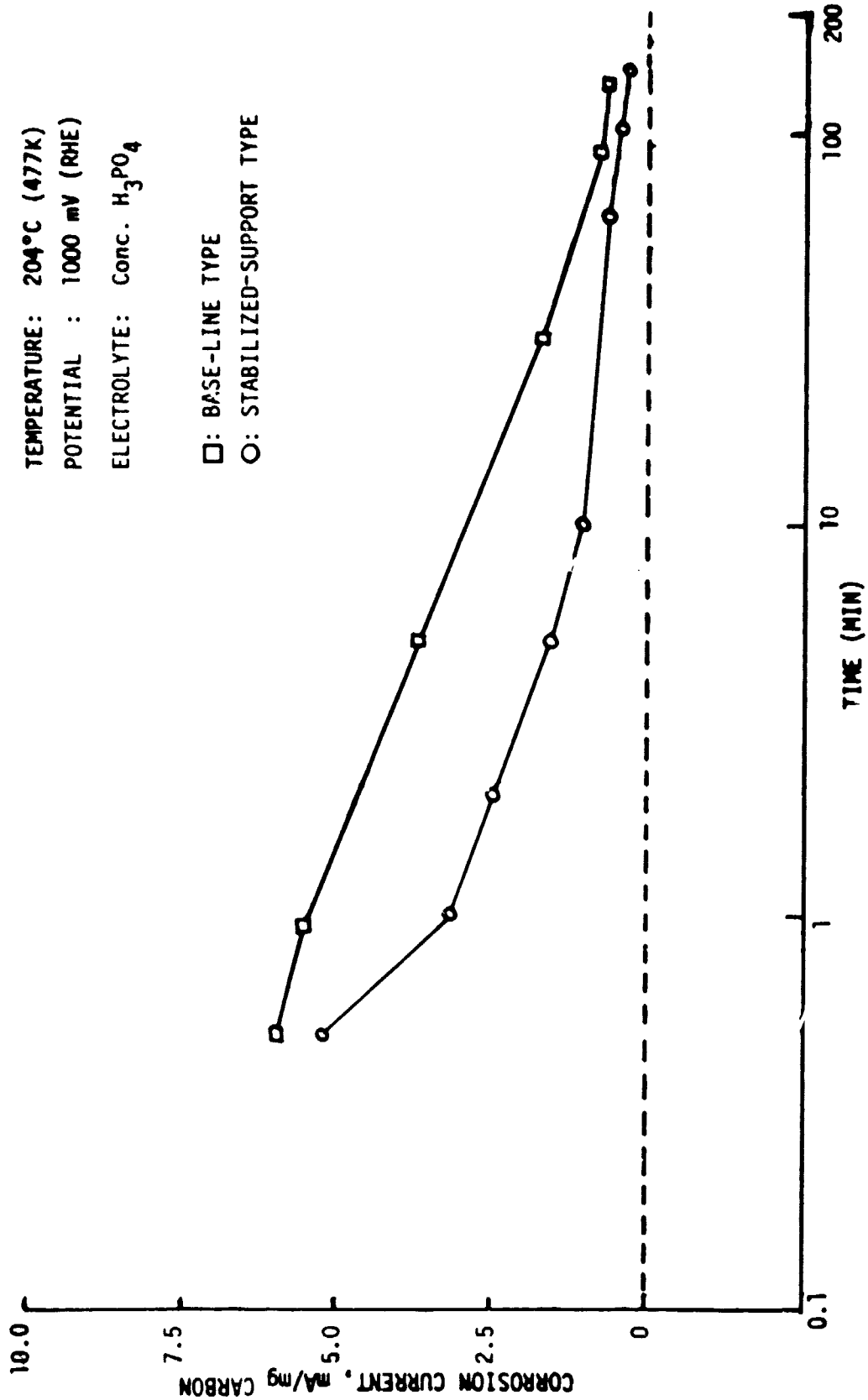

FIGURE 18 CORROSION CURRENTS OF CARBON-SUPPORTED ELECTROCATALYSTS

ENGELHARD

ORIGINAL PAGE IS
OF POOR QUALITY

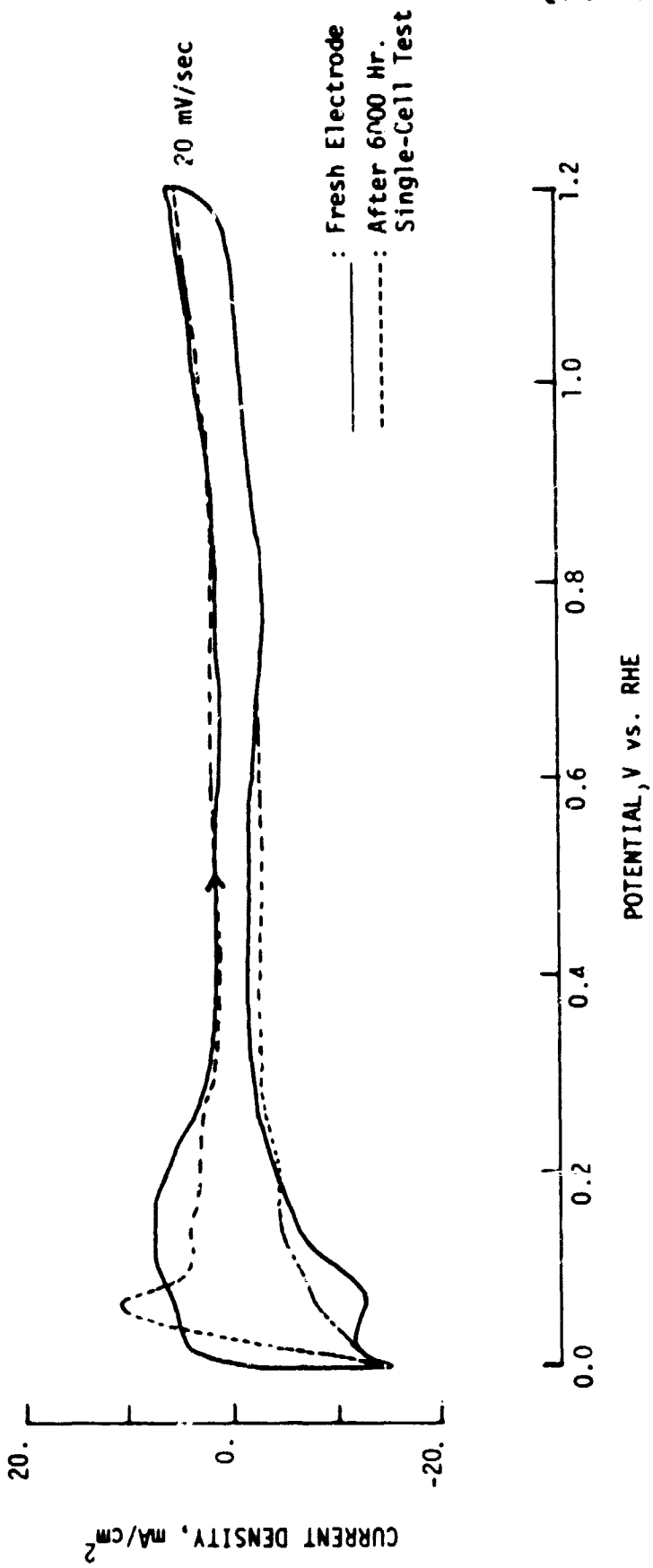

FIGURE 19 CYCLIC-VOLTAMMOGRAMS FOR STABILIZED-Pt/STABILIZED-SUPPORT TYPE ELECTROCATALYST (11175-33-2) IN 25% H_3PO_4 AT 25°C (298K)

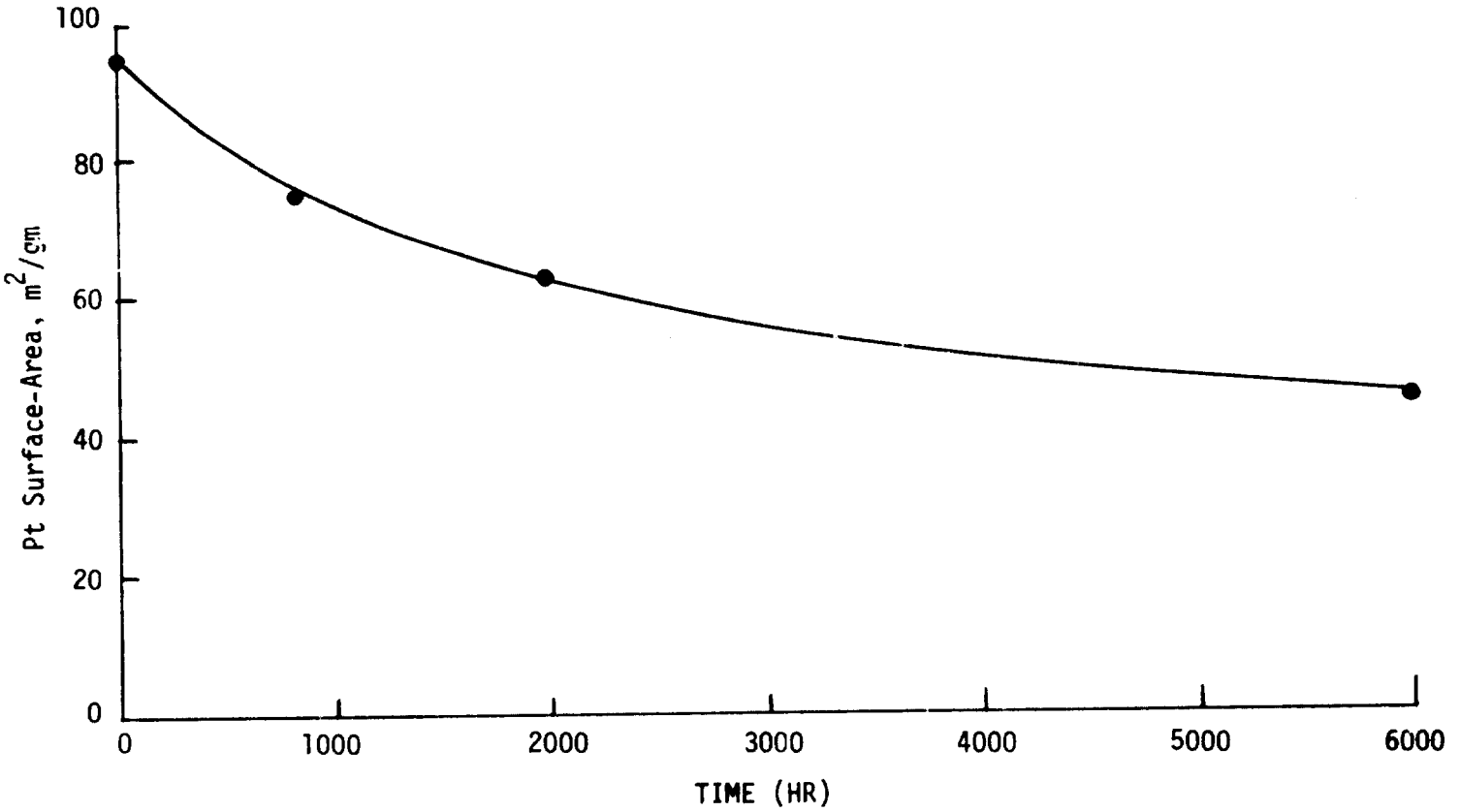

FIGURE 20 Pt SURFACE-AREA LOSS FOR STABILIZED-Pt/STABILIZED-SUPPORT TYPE ELECTROCATALYST (11175-33-2) DURING CELL OPERATION

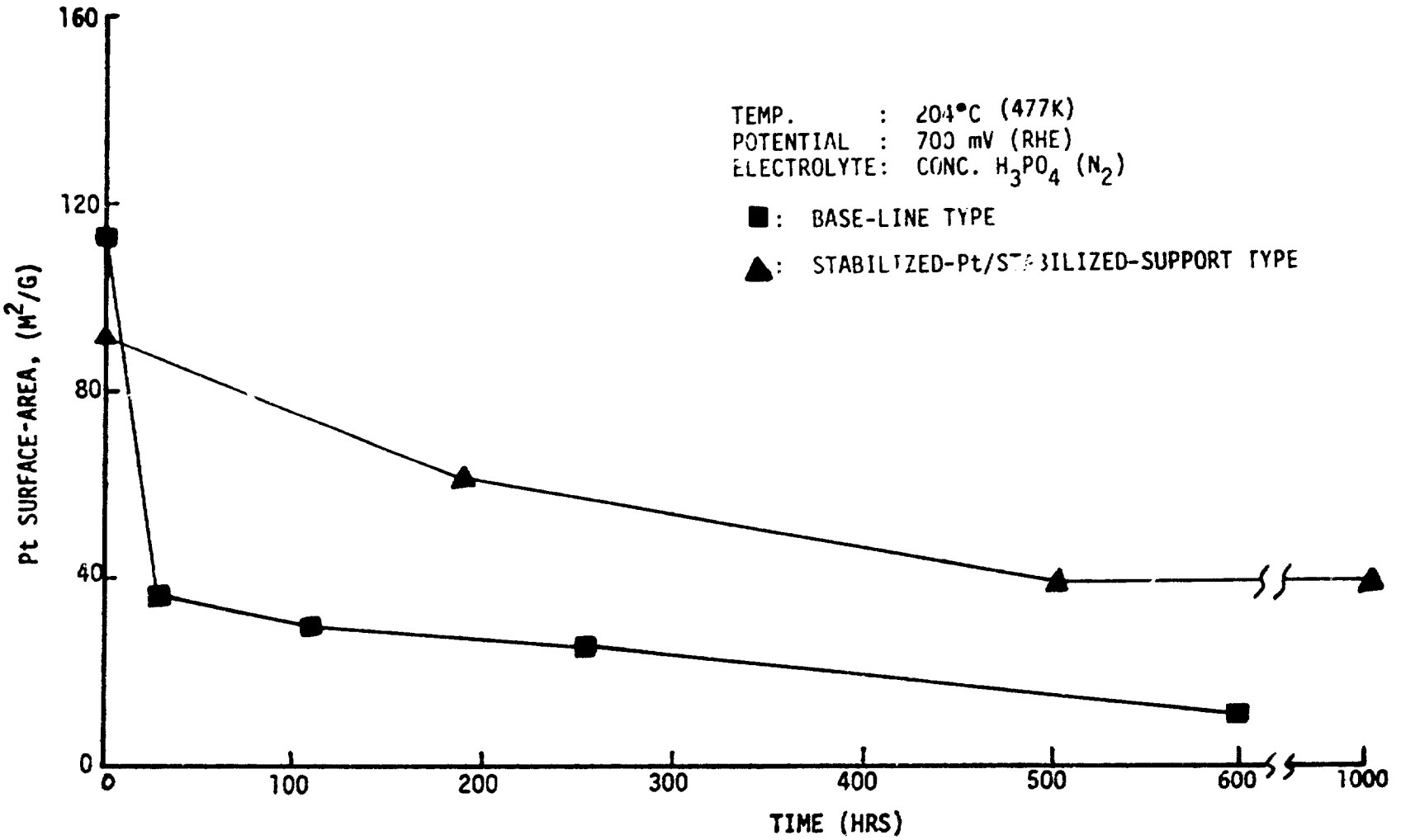

FIGURE 21 PLATINUM SURFACE-AREA LOSS UNDER POTENTIOSTATIC AGING CONDITIONS

ENGELHARD

ORIGINAL PAGE IS
OF POOR QUALITY

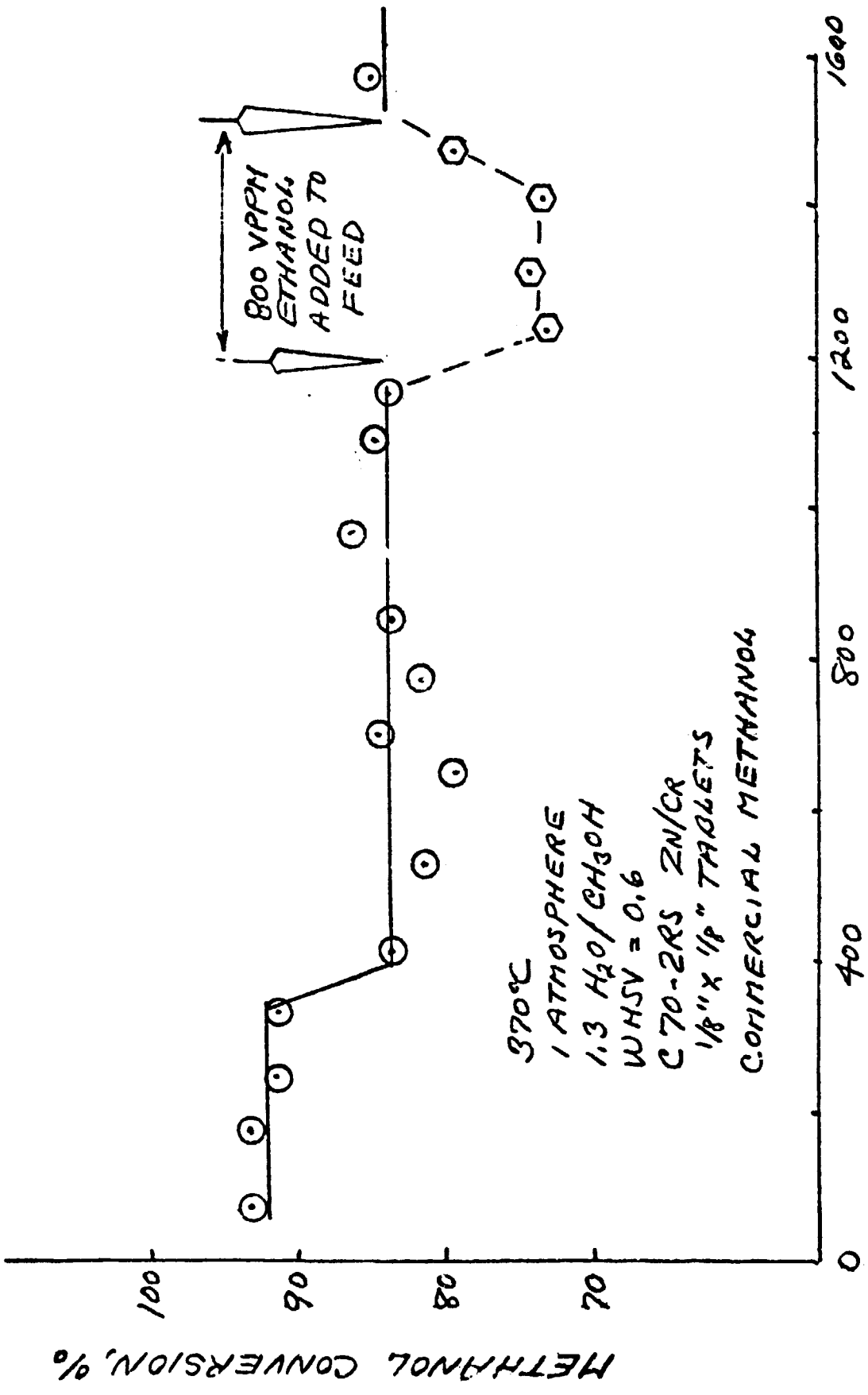

FIGURE 22 AGING TEST OF CATALYST C70-2RS, METHANOL/STEAM REFORMING